Pleiotropic regulation of renal sodium handling by the circadian clock

Svetlana Nikolaeva[1,2], Sylvain Pradervand[4,5], Gabriel Centeno[1], Vlasta Zavadova[1], Natsuko Tokonami[1], Marc Maillard[3], Olivier Bonny[1,3] and Dmitri Firsov[1]

[1] - Department of Pharmacology and Toxicology, University of Lausanne, Switzerland

[2] - Institute of Evolutionary Physiology and Biochemistry, St-Petersburg, Russia

[3] – Service of Nephrology, Department of Medicine, CHUV, Lausanne, Switzerland

[4] – Genomic Technologies Facility, University of Lausanne, Switzerland

[5] – Swiss Institute of Bioinformatics, Lausanne, Switzerland

to whom correspondence should be addressed:

Dmitri FIRSOV

Department of Pharmacology and Toxicology, University of Lausanne, 27 rue du Bugnon, 1005 Lausanne, Switzerland

Phone: ++ 41-216925406 Fax: ++ 41-216925355 e-mail: dmitri.firsov@unil.ch

running title: circadian clock in the kidney

word count: abstract: 174 words; text: 2919 words

The circadian clock is involved in the control of blood pressure. However, the underlying mechanisms remain unclear. Here we analyzed circadian rhythms in kidneys of wild-type mice and mice lacking the circadian transcriptional activator *clock*. We show that *clock*(-/-) mice exhibit dramatic changes in circadian rhythm of renal sodium excretion. In parallel, the normal circadian rhythmicity of plasma aldosterone levels is lost in *clock*(-/-) mice. Analysis of renal circadian transcriptomes demonstrated deep changes in multiple mechanisms involved in maintaining sodium balance. Pathway analysis revealed the strongest effect on the enzymatic system involved in the formation of 20-HETE, a powerful regulator of renal sodium excretion, renal vascular tone and blood pressure. This correlated with a significant decrease in the renal and urinary content of 20-HETE in *clock*(-/-) mice. This study reveals a pleiotropic effect of circadian clock on renal function and identifies the 20-HETE synthesis pathway as one of its principal renal targets. It also suggests that the circadian clock regulates blood pressure, at least in part, by exerting dynamic control over renal sodium handling.

Recent evidence indicates that the circadian clock is involved in blood pressure control. In mice, suppression or decrease of the circadian clock activity via deletion of the circadian transcriptional activators Bmal1, Clock or Npas2 leads to low blood pressure, whereas its constitutive activation via deletion of the circadian repressors Cry1and Cry2 results in salt-sensitive hypertension.[1-4] Wang et al, have recently shown that mice simultaneously devoid of three PAR b-Zip circadian transcriptional factors Dbp, Hlf and Tef exhibit a significant reduction in blood pressure.[5] Maintaining blood pressure within normal range strongly depends on the capacity of the kidney to precisely regulate sodium content in the extracellular space. Thus, dysregulation of molecular mechanisms involved in renal sodium handling could be partially responsible for the elevated or decreased blood pressure observed in mice with genetically altered clocks. This hypothesis is supported by evidence in humans suggesting that alteration of circadian rhythms of urinary sodium excretion is the primary cause of disease in several forms of hyper- or hypo- tension. For instance, a decreased renal capacity to excrete sodium during the daytime has been shown to correlate with nocturnal hypertension, whereas an increased sodium excretion during the nighttime contributes to the maintenance of orthostatic hypotension.[6,7] Importantly, significant changes in the amplitude and/or the circadian phase of urinary excretion of sodium can be provoked not only by a pathological process but also by a misalignment between the endogenous circadian clock and the imposed rest-activity or feeding cycles, or by sleep disturbance. For instance, Kamperis et al. have shown that acute sleep deprivation in humans leads to excessive natriuresis and kaliuresis during the subjective night and attenuation of the nocturnal blood pressure dip.[8] Numerous studies have demonstrated an impairment of the sodium excretory rhythm and the development of hypertension in shift workers.[9,10]

It has been shown that circadian clock can influence renal function via two types of circadian inputs: (i) via entrainment of renal rhythms through the external circadian time cues

such as hormones, food, activity and body temperature rhythms and, (ii) via the activity of the intrinsic renal circadian clock. For instance, Doi et al. have shown that the circadian timing system controls sodium reabsorption in the distal nephron and the collecting duct via an effect on the aldosterone production in the adrenal glands.[3] On the other hand, Saifur Rohman et al. have demonstrated that the intrinsic renal clock directly regulates the activity of the Na^+/H^+ exchanger NHE3 in the proximal tubule[11] and, Gumz et al. have shown that the circadian repressor PER1 is capable of regulating the epithelial sodium channel (ENaC) expression in the collecting duct cells.[12] We have recently demonstrated that the molecular clocks in the distal nephron and the collecting duct display robust circadian oscillations and that mice devoid of the *clock* gene exhibit a significant reduction in blood pressure.[2] However, the relationship between the circadian clock activity and the rhythms of electrolyte excretion in the urine has not been established. Also, a systematic analysis of circadian mechanisms involved in maintaining electrolyte balance is still lacking.

To address these questions we studied functional and molecular aspects of urine excretory rhythms in wild-type mice and mice devoid of the *clock* gene. This model was selected because the CLOCK is essential for the rhythmicity of peripheral molecular oscillators but is not required for circadian behavior.[13,14] The latter fact allows for minimizing the interference of confounding factors such as changes in the circadian patterns of food and water intake or locomotor activity.[2]

RESULTS

Circadian rhythms of urinary sodium and potassium excretion in wild-type and clock–knockout mice All mice were adapted to a 12 hour light and 12 hour dark cycle (LD) for two weeks. To exclude the influence of light on urinary rhythms, half the animals were placed in constant darkness (DD) 30 hours before urine collection. Hourly collection of urine was performed from freely moving mice housed individually in the metabolic cages (see Methods). As shown in Figure 1A, wild-type mice in LD conditions exhibited a well-marked circadian rhythm of sodium excretion with the maximal values in the first half of the activity phase (time is expressed in ZT or Zeitgeber time units; ZT0 is the time of light-on and ZT12 is the time of light-off) and a trough during the inactive phase. This rhythm was maintained under DD conditions, with the exception of three time-points (CT0, CT10 and CT18 (CT, circadian time, indicates the subjective circadian time independent of a zeitgeber)) where the difference between the LD and DD conditions was statistically significant (Figure 1A). In *clock*(-/-) mice the difference between the amounts of sodium excreted during the light and dark phases (or subjective light and dark phases in DD conditions) was apparently reduced in both LD and DD conditions (Figure 1B). For the quantitative assessment of the difference we calculated the ratio between the amounts of sodium excreted between ZT0 and ZT12, and ZT12 and ZT24, or CT0 and CT12, and CT12 and CT24 in LD and DD conditions, respectively. As shown in Figure 1C, the ratio was significantly increased in *clock*(-/-) mice, in both LD and DD conditions. Similar results were obtained for the rhythms of urinary potassium excretion (Supplementary Figure1). The urinary excretion rates for sodium and potassium were higher in *clock*(-/-) mice; however, this difference reached statistical significance only for the sodium excretion rate in LD conditions (Table 1). In parallel, there was a tendency for increased food and water intake in *clock*-knockout mice in DD conditions; however, the statistical significance was reached only for the water intake (Table 1).

Plasma aldosterone levels in wild-type and clock-knockout mice To check whether changes in the renin-angiotensin-aldosterone system may contribute to the impairment of sodium and potassium excretory rhythms in *clock*(-/-) mice we performed an analysis of plasma aldosterone levels in blood samples collected every 4 hours during a 24-hour period (6 time-points). As shown in Figure 2, aldosterone levels in wild-type mice vary between time points (p=0.003, one-way ANOVA) and follow a circadian temporal pattern with maximum at ZT12, the time of transition from the inactive to the active phase of the circadian cycle (fitted to the cosine function with p=0.007). Circadian fit was performed using a linear model with a pair of cosine and sine functions as the explanatory variable, with the frequency corresponding to 24-hour periodicity as described previously (2). A similar circadian pattern of plasma aldosterone levels has been previously described in humans[15,16] and rats.[17] In *clock*(-/-) mice, although differences were still observed between time points (p=0.026, one-way ANOVA), the circadian pattern was disrupted (fitted to the cosine function with p=0.183) and a significant difference with plasma aldosterone levels in wild-type mice at ZT12 was observed. However, the 24-hour mean of plasma aldosterone levels was not different between the wild-type and *clock*(-/-) mice (260.3±22.1 pg/ml vs.250.8±27.4 pg/ml, respectively, p=0.7, two-way ANOVA). Also, there was no difference of urinary Na^+/K^+ ratio, an indicator of plasma aldosterone activity (with the exception of ZT23 in LD conditions for which the difference was statistically significant ($p<0.05$), Supplementary Figure 2).

Comparison of whole-kidney transcriptomes of wild-type and clock-knockout mice To identify molecular mechanisms underlying sodium and potassium excretory rhythms, we

performed circadian profiling of renal transcriptomes in wild-type and *clock*(-/-) mice. The RNA was extracted from whole kidneys of mice adapted to LD conditions for two weeks and then placed in constant darkness (DD) for 30 hours before sacrifice. Mice were sacrificed every 4 hours over the course of circadian cycle. Hybridization data were analyzed with two distinct statistical protocols (see Supplementary Methods). *First*, circadian oscillatory transcripts were identified independently in wild-type and *clock*(-/-) mice by fitting their temporal expression profiles to a cosine function with a period of 24 hours. A total of 277 and 174 transcripts in kidneys of wild-type and *clock*(-/-) mice met these criteria, respectively (Supplementary Tables 1 and 3 respectively; false discovery rate (FDR) < 0.1). Importantly, all principal elements of positive and negative limbs of molecular clock (Bmal1 (*Arntl*), Clock, Npas2, Cry1, Cry2, Per1, Per2, Per3 and Rev-erb alpha (*Nr1d1*)) were identified as circadian transcripts in the kidneys of wild-type mice (Supplementary Table 1). For most of these genes the circadian amplitude was significantly reduced in *clock*(-/-) mice (Figures 3A and 3B). The whole-transcriptome distribution of acrophases was also significantly modified in *clock*(-/-) mice (Figure 3C). Analysis of circadian genes in wild-type mice revealed a large number of transcript encoding proteins involved in various transcellular or paracellular transport functions: the amino acid transporters (Slc6a20a, Slc6a19 and Slc7a8), the monocarboxylate transporter 1 (Slc16a1), the Na^+-dependent bile acid transporter (Slc10a2), the urate transporter (Slc2a9), the nucleoside transporter (slc29a3), claudins 1 and 10, the sodium/proton exchanger 3 (NHE3/Slc9a3), serine/threonine kinases Sgk1 and Sik1, nuclear receptors Thrα and Pparα, modulators of distal sodium reabsorption Usp2 and Gilz (Tsc22d3) and enzymes involved in the synthesis/degradation of autocrine/paracrine regulators of sodium reabsorption and potassium secretion (thromboxane synthase (Tbxas1), dopamine decarboxylase (DDC) and catechol-O-methyltransferase (COMT1)) (Supplementary Table 1). Interestingly, most of these transcripts did not meet the criteria for

circadian oscillations in *clock*(-/-) mice and the amplitudes of their diurnal variations were significantly reduced (with the exception of Gilz and Slc6a20a, Figures 3A and 3B, Supplementary Table 2). Because the cosinor statistical treatment is applicable only to transcripts fitting to the cosine function, we also applied a *second* data analysis approach to identify genes differentially expressed between the *clock*(-/-) and wild-type kidneys irrespective of their temporal expression patterns. As shown in Supplementary Table 3, 36 and 43 transcripts are up- or down- regulated in kidneys of *clock*(-/-) mice, respectively (fold change > 50%, FDR<0.1). Interestingly, several of these transcripts (Cyp4a12a, Cyp4a12b, Cyp4a14, Cyp2c44 and Cyp2j13) encode enzymes involved in the conversion of arachidonic acid to different active metabolites. Three enzymes Cyp4a12a, Cyp4a12b and Cyp4a14 are required for the oxidation of arachidonic acid to 20-hydroxyeicosatetraenoic acid (20-HETE), a powerful endogenous regulator of renal sodium reabsorption and potassium secretion and of the renal vascular tone. Pathway enrichment analysis performed on the up-and down- regulated transcripts confirmed a strong enrichment in transcripts involved in the arachidonic acid conversion pathways (10.8-fold enrichment, FDR=0.004, Supplementary Table 4). To validate the microarray results, real-time PCR was performed for the CYPs involved in the synthesis of 20-HETE on independent samples of RNA extracted from the kidneys of 30 wild-type and 30 *clock(-/-)* mice (5 mice/time-point). As shown in Figure 4A, 4B and 4C, the 24-hour mean expression levels of Cyp4a12a and Cyp4a12b are significantly decreased whereas the expression level of Cyp4a14 is significantly increased in kidneys of *clock(-/-)* mice, thereby confirming the results of the microarray analysis (see panels A, B and C in Supplementary Figure 3, respectively, and Supplementary Table 3). However, the temporal patterns of Cyp4a12a, Cyp4a12b and Cyp4a14 RNA expression were significantly different between the microarray analysis (see panels D, E and F in Supplementary Figure, respectively) and the real-time PCR amplification (Figure 4D, 4E and 4F, respectively). A

possible explanation for this difference is that the members of the CYP4a subfamily share a high degree of nucleotide identity (e.g. 98% of nucleotide identity between Cyp4a12a and Cyp4a12b, see Supplementary Table 5). The high degree of sequence homology is a known source of errors in microarray analysis resulting from the cross-hybridization of related transcripts. In LD condition, the changes in the expression levels of Cyp4a12a, Cyp4a12b and Cyp4a14 in clock(-/-) mice were similar to those observed in DD condition (Supplementary Figure 4).

Assessment of 20-HETE levels To determine whether renal content of 20-HETE is modified in *clock*(-/-) mice, we performed a quantitative analysis of this metabolite in renal microsomes and in the urine. As shown in Figure 5A, in both wild-type and *clock*(-/-) mice, 20-HETE levels in microsomes change across time points ($p=0.007$ and $p=0.004$, respectively, one-way ANOVA) and follow a circadian-like temporal pattern (fitted to the cosine function with $p<0.001$ for wild-type and *clock*(-/-) mice). However, 20-HETE oscillations in *clock*(-/-) mice exhibit a significant shift in the acrophase (acrophase at CT20 in wild-type mice vs. acrophase at CT12 in *clock*(-/-) mice) and a significant decrease in the 24-hour mean 20-HETE levels ($p=0.023$, two-way ANOVA, Figure 5B). A similar decrease was observed in the 24-hour mean 20-HETE levels in the urine of *clock*(-/-) mice (Figure 5C).

DISCUSSION

The results of our study indicate that the circadian timing system controls the daily rhythms of sodium and potassium excretion by the kidney and suggests that dysfunction of these rhythms may have a significant influence on blood pressure.

Analysis of *clock*(-/-) mice revealed several mechanisms by which the circadian timing system controls sodium and potassium excretion by the kidney: *(i)* We demonstrated that the normal circadian rhythmicity of plasma aldosterone levels is lost in *clock*(-/-) mice. Because aldosterone is the principal hormone controlling sodium reabsorption in the distal nephron and the collecting duct, these changes are expected to have a direct influence on the dynamic of sodium excretion by the kidney. Interestingly, the 24-hour mean aldosterone levels were not different between the wild-type and *clock*(-/-) mice. These results are surprising because genetic ablation of the circadian transcriptional factors *dbp, hlf* and *tef* results in a significant decrease of plasma aldosterone levels[5] whereas mice devoid of *cry1* and *cry2* display primary hyperaldosteronism.[3] This indicates that the different elements of the circadian clock have a different impact on the aldosterone synthesis and/or secretion. *(ii)* Cosinor analysis of renal transcriptomes revealed a large number of circadian transcripts that encode proteins involved in tubular reabsorption/secretion of various substrates, including sodium and potassium. In *clock*(-/-) mice, circadian rhythmicity of most of these transcripts was lost. One of these transcripts encodes the sodium-proton exchanger NHE3, a transporter that is directly regulated by the circadian clock.[11] Importantly, NHE3 is the major transporter mediating sodium reabsorption in the proximal tubule and mice devoid of the *NHE3* gene exhibit mild hypotension.[18] Another interesting transcript is Sgk1, a serine-threonine kinase that regulates a variety of sodium transporters all along the renal tubule. Bozek et al., have recently proposed that this kinase is also directly regulated by the circadian clock.[19] These two examples clearly demonstrate that the

impairment of renal sodium handling in *clock*(-/-) mice might be directly related to the dysfunction in the intrinsic renal clock. *(iii)* Our study reveals a major role of the circadian timing system in the regulation of the expression of renal cytochrome p450 enzymes involved in the formation of 20-HETE, a powerful mediator of blood pressure control by the kidney (reviewed in [20-22]). In parallel, we demonstrate that the renal content of 20-HETE exhibits a clear circadian pattern and that this pattern is significantly modified in kidneys of *clock*(-/-) mice. 20-HETE has a potent pro-hypertensive effect by acting as a vasoconstrictor of preglomerular arterioles, but it is also capable of inhibiting several important sodium transporters in the proximal tubule and the thick ascending limb (Na^+-K^+-ATPase, NHE3, NKCC2),[23-26] thereby promoting sodium excretion and lowering the blood pressure. 20-HETE is mainly produced by Cyp4a subfamily of enzymes located in both, microvessels and tubular cells. Disruption of Cyp4a14 gene in mice causes gender-specific hypertension in males, which results from the increased plasma androgen levels and up-regulation of androgen-sensitive Cyp4a12 *a* and *b* isoforms, the predominant 20-HETE synthases in the male mouse kidney.[27] Holla et al. proposed that Cyp4a12-mediated increase in renal 20-HETE levels is responsible for hypertension in Cyp4a14-knockout mice.[28] This mechanism seems to mirror our findings in *clock*(-/-) mice. Indeed, the increase in Cyp4a14 expression levels and the decrease in Cyp4a12a and Cyp4a12b expression levels in *clock*(-/-) mice correlates with the lower renal content of 20-HETE and decreased blood pressure. We propose that the changes in the renal content of 20-HETE could be one of the possible causes in the dysfunction of the renal excretory rhythms and blood pressure control in *clock*(-/-) mice. Our findings that 20-HETE levels in the kidney exhibit circadian rhythms may have clinical importance. Indeed, drugs targeting the 20-HETE axis present an interesting therapeutic potential for vascular and salt-sensitive hypertension, acute kidney injury and renal cancer.[22,29,30] Some of such compounds are currently being tested in preclinical studies.[22] The circadian rhythmicity of

20-HETE levels indicates that the safety and efficiency of these drugs could be variable depending on the time they are administrated.

METHODS

Animals A colony of *clock* deficient mice was established from breeding pairs of *clock*(+/-) heterozygous mice originally generated by Debruyne et al.[13] The *clock*(+/-) mice were backcrossed to C57BL/6J mice for >9 generations. All experiments with animals were performed in accordance with the Swiss guidelines for animal care which conform to the National Institutes of Health animal care guidelines. Animals were fed with a standard mouse diet (#3800) from KLIBA (Kaiseraugst, Switzerland). This diet contains 0.23% of sodium (see: www.kliba-nafag.ch).

Urine collection Mice were housed in individual metabolic cages (Tecniplast, Italy). Urine collection was performed after a 3-day adaptation period. Hourly urine collection was simultaneously obtained from 6 wild-type and 6 knockout mice with the help of a 12-channel peristaltic pump (IPC, Ismatec, Switzerland) connected to a fraction collector (FC204, Gilson, Switzerland). Both the peristaltic pump and the fraction collector were automatically switched on every hour for two minutes. This protocol rendered unnecessary the experimenter's presence during the 24-hour collection period. Urine was collected under mineral oil to avoid evaporation. Urine content of sodium and potassium was determined by flame photometry.

Analysis of plasma aldosterone levels Plasma aldosterone was measured by a conventional radioimmunoassay (DPC, USA). All blood samples were collected retro-orbitally and stored on ice.

Analysis of 20-HETE levels 20-HETE levels were measured using Detroit R&D kits. Microsomes were prepared according to the manufacturer's protocol (Detroit R&D).

ACKNOWLEDGMENTS We thank David Weaver (University of Massachusetts Medical School, MA) for the generous gift of the *clock* deficient mice and Otto Hagenbuchle, Keith Harshman, Alexandra Paillusson and Mélanie Dupasquier from Lausanne Genomic Technologies Facility for the microarray profiling studies. This work was supported by the Swiss National Science Foundation research grant 31003A-132496 (to D.F.)

FIGURE LEGENDS

Figure 1. **A.** Temporal profile of renal sodium excretion rates in wild-type mice in LD or DD conditions. **B.** Temporal profile of renal sodium excretion rates in *clock(-/-)* mice in LD or DD conditions. **C.** Ratio between sodium excreted during the day (ZT0-ZT12) and the night (ZT12-ZT24) in LD conditions or during the subjective day (CT0-CT12) and subjective night (CT12-CT24) in DD conditions. Values are averages ±SEM from n=11 mice. Statistical significance was calculated using unpaired *t*-test. *, $p<0.05$, (n=11).

Figure 2. Temporal profiles of plasma aldosterone levels in wild-type (black bars) and *clock*(-/-) mice (white bars). Values are means ±SEM from n=5 mice. Statistical significance was calculated using unpaired *t*-test. *, $p<0.05$

Figure 3. Deletion of the *clock* gene affects circadian patterns of gene expression in the kidney. **A.** Phase ordering of 277 genes oscillating in wild-type mice: on the left: wild-type transcripts; on

the right: *clock*(-/-) transcripts. The temporal expression of the *clock* gene is shown in the enlargement. Green and red represent minimal and maximal expression levels, respectively. The time of maximal transcript expression (acrophase) is indicated on the left. **B.** Oscillating transcripts shown in **A** are plotted according to their amplitude and phase in wild-type and *clock*(-/-) mice. Principal elements of molecular clock are indicated in black. **C.** Density distribution of acrophases for all the 28,220 transcripts tested on microarrays in wild-type and *clock*(-/-) mice.

Figure 4. Expression levels of Cyp4a12a, Cyp4a12b and Cyp4a14 transcripts in kidneys of wild-type and *clock*(-/-) mice. Panels A, B and C show qPCR-based quantitation of 24-hour mean expression levels of Cyp4a12a, Cyp4a12b and Cyp4a14, respectively. Values are means ±SEM from n=30 mice. Panels D, E and F represent qPCR-based temporal profiling of Cyp4a12a, Cyp4a12b and Cyp4a14 RNA expression in kidneys of wild-type (black line) and *clock*(-/-) (grey line) mice, respectively. Values are means ±SEM from n=5 mice. ***, $p<0.001$, two-way ANOVA.

Figure 5. A. Temporal profiles of 20-HETE levels in kidney microsomes of wild-type (black lane) and *clock*(-/-) mice (grey lane) . Values are means ±SEM from n=6 mice. **B.** 24-hour mean 20-HETE levels in kidney microsomes. Values are means ±SEM from n=35 mice. *, $p<0.05$, two-way ANOVA. **C.** 24-hour mean 20-HETE levels in the urine of wild-type and *clock*(-/-) mice. Values are means ±SEM from n=6 mice. *, $p<0.05$, *t*-test.

REFERENCES

1. Curtis AM, Cheng Y, Kapoor S, Reilly D, Price TS, Fitzgerald GA: Circadian variation of blood pressure and the vascular response to asynchronous stress. *Proc Natl Acad Sci U S A* 104**:** 3450-3455, 2007
2. Zuber AM, Centeno G, Pradervand S, Nikolaeva S, Maquelin L, Cardinaux L, Bonny O, Firsov D: Molecular clock is involved in predictive circadian adjustment of renal function. *Proc Natl Acad Sci U S A* 106**:** 16523-16528, 2009
3. Doi M, Takahashi Y, Komatsu R, Yamazaki F, Yamada H, Haraguchi S, Emoto N, Okuno Y, Tsujimoto G, Kanematsu A, Ogawa O, Todo T, Tsutsui K, van der Horst GT, Okamura H: Salt-sensitive hypertension in circadian clock-deficient Cry-null mice involves dysregulated adrenal Hsd3b6. *Nat Med* 16**:** 67-74, 2009
4. Rudic RD, Fulton DJ: Pressed for time: the circadian clock and hypertension. *J Appl Physiol* 107**:** 1328-1338, 2009
5. Wang Q, Maillard M, Schibler U, Burnier M, Gachon F: Cardiac hypertrophy, low blood pressure, and low aldosterone levels in mice devoid of the three circadian PAR bZip transcription factors DBP, HLF, and TEF. *Am J Physiol Regul Integr Comp Physiol* 299**:** R1013-1019, 2010
6. Pechere-Bertschi A, Nussberger J, Biollaz J, Fahti M, Grouzmann E, Morgan T, Brunner HR, Burnier M: Circadian variations of renal sodium handling in patients with orthostatic hypotension. *Kidney Int* 54**:** 1276-1282, 1998
7. Burnier M, Coltamai L, Maillard M, Bochud M: Renal sodium handling and nighttime blood pressure. *Semin Nephrol* 27**:** 565-571, 2007
8. Kamperis K, Hagstroem S, Radvanska E, Rittig S, Djurhuus JC: Excess diuresis and natriuresis during acute sleep deprivation in healthy adults. *Am J Physiol Renal Physiol* 299**:** F404-411, 2010
9. Suwazono Y, Dochi M, Sakata K, Okubo Y, Oishi M, Tanaka K, Kobayashi E, Nogawa K: Shift work is a risk factor for increased blood pressure in Japanese men: a 14-year historical cohort study. *Hypertension* 52**:** 581-586, 2008
10. Conroy RT, Elliott AL, Mills JN: Circadian excretory rhythms in night workers. *Br J Ind Med* 27**:** 356-363, 1970
11. Saifur Rohman M, Emoto N, Nonaka H, Okura R, Nishimura M, Yagita K, van der Horst GT, Matsuo M, Okamura H, Yokoyama M: Circadian clock genes directly regulate expression of the Na(+)/H(+) exchanger NHE3 in the kidney. *Kidney Int* 67**:** 1410-1419., 2005
12. Gumz ML, Stow LR, Lynch IJ, Greenlee MM, Rudin A, Cain BD, Weaver DR, Wingo CS: The circadian clock protein Period 1 regulates expression of the renal epithelial sodium channel in mice. *J Clin Invest* 119**:** 2423-2434, 2009
13. Debruyne JP, Noton E, Lambert CM, Maywood ES, Weaver DR, Reppert SM: A clock shock: mouse CLOCK is not required for circadian oscillator function. *Neuron* 50**:** 465-477., 2006
14. DeBruyne JP, Weaver DR, Reppert SM: Peripheral circadian oscillators require CLOCK. *Curr Biol* 17**:** R538-539, 2007
15. Rittig S, Matthiesen TB, Pedersen EB, Djurhuus JC: Circadian variation of angiotensin II and aldosterone in nocturnal enuresis: relationship to arterial blood pressure and urine output. *J Urol* 176**:** 774-780, 2006
16. Hurwitz S, Cohen RJ, Williams GH: Diurnal variation of aldosterone and plasma renin activity: timing relation to melatonin and cortisol and consistency after prolonged bed rest. *J Appl Physiol* 96**:** 1406-1414. Epub 2003 Dec 1405., 2004
17. Hilfenhaus M: Circadian rhythm of the renin-angiotensin-aldosterone system in the rat. *ArchTox* 36**:** 305-316, 1976
18. Schultheis PJ, Clarke LL, Meneton P, Miller ML, Soleimani M, Gawenis LR, Riddle TM, Duffy JJ, Doetschman T, Wang T, Giebisch G, Aronson PS, Lorenz JN, Shull GE: Renal and intestinal absorptive defects in mice lacking the NHE3 Na+/H+ exchanger. *Nat Genet* 19**:** 282-285, 1998
19. Bozek K, Relogio A, Kielbasa SM, Heine M, Dame C, Kramer A, Herzel H: Regulation of clock-controlled genes in mammals. *PLoS One* 4**:** e4882, 2009
20. Hao CM, Breyer MD: Physiologic and pathophysiologic roles of lipid mediators in the kidney. *Kidney Int* 71**:** 1105-1115, 2007
21. Capdevila JH: Regulation of ion transport and blood pressure by cytochrome p450 monooxygenases. *Curr Opin Nephrol Hypertens* 16**:** 465-470, 2007
22. Williams JM, Murphy S, Burke M, Roman RJ: 20-hydroxyeicosatetraeonic acid: a new target for the treatment of hypertension. *J Cardiovasc Pharmacol* 56**:** 336-344, 2010
23. Ominato M, Satoh T, Katz AI: Regulation of Na-K-ATPase activity in the proximal tubule: role of the protein kinase C pathway and of eicosanoids. *J Membr Biol* 152**:** 235-243, 1996

24. Yu M, Lopez B, Dos Santos EA, Falck JR, Roman RJ: Effects of 20-HETE on Na+ transport and Na+ -K+ -ATPase activity in the thick ascending loop of Henle. *Am J Physiol Regul Integr Comp Physiol* 292**:** R2400-2405, 2007
25. Quigley R, Chakravarty S, Zhao X, Imig JD, Capdevila JH: Increased renal proximal convoluted tubule transport contributes to hypertension in Cyp4a14 knockout mice. *Nephron Physiol* 113**:** p23-28, 2009
26. Amlal H, Legoff C, Vernimmen C, Paillard M, Bichara M: Na(+)-K+(NH4+)-2Cl- cotransport in medullary thick ascending limb: control by PKA, PKC, and 20-HETE. *Am J Physiol* 271**:** C455-463, 1996
27. Muller DN, Schmidt C, Barbosa-Sicard E, Wellner M, Gross V, Hercule H, Markovic M, Honeck H, Luft FC, Schunck WH: Mouse Cyp4a isoforms: enzymatic properties, gender- and strain-specific expression, and role in renal 20-hydroxyeicosatetraenoic acid formation. *Biochem J* 403**:** 109-118, 2007
28. Holla VR, Adas F, Imig JD, Zhao X, Price E, Jr., Olsen N, Kovacs WJ, Magnuson MA, Keeney DS, Breyer MD, Falck JR, Waterman MR, Capdevila JH: Alterations in the regulation of androgen-sensitive Cyp 4a monooxygenases cause hypertension. *Proc Natl Acad Sci U S A* 98**:** 5211-5216, 2001
29. Hoff U, Lukitsch I, Chaykovska L, Ladwig M, Arnold C, Manthati VL, Fuller TF, Schneider W, Gollasch M, Muller DN, Flemming B, Seeliger E, Luft FC, Falck JR, Dragun D, Schunck WH: Inhibition of 20-HETE synthesis and action protects the kidney from ischemia/reperfusion injury. *Kidney Int* 79**:** 57-65, 2011
30. Panigrahy D, Kaipainen A, Greene ER, Huang S: Cytochrome P450-derived eicosanoids: the neglected pathway in cancer. *Cancer Metastasis Rev* 29**:** 723-735, 2010

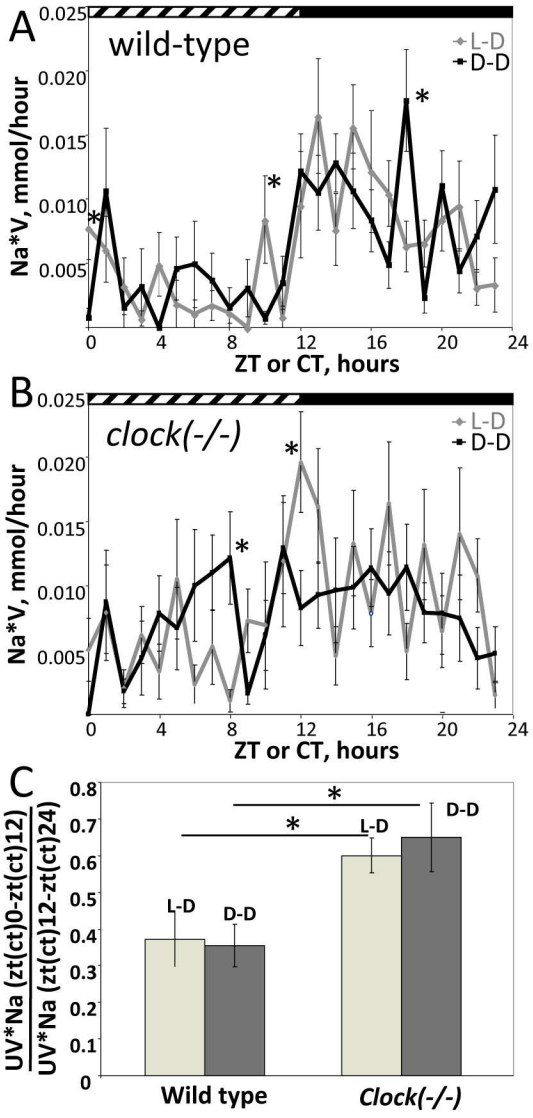

Nikolaeva et al., Figure 1

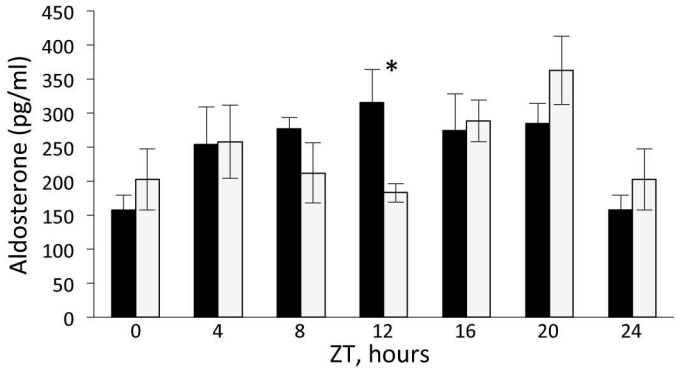

Nikolaeva et al., Figure 2

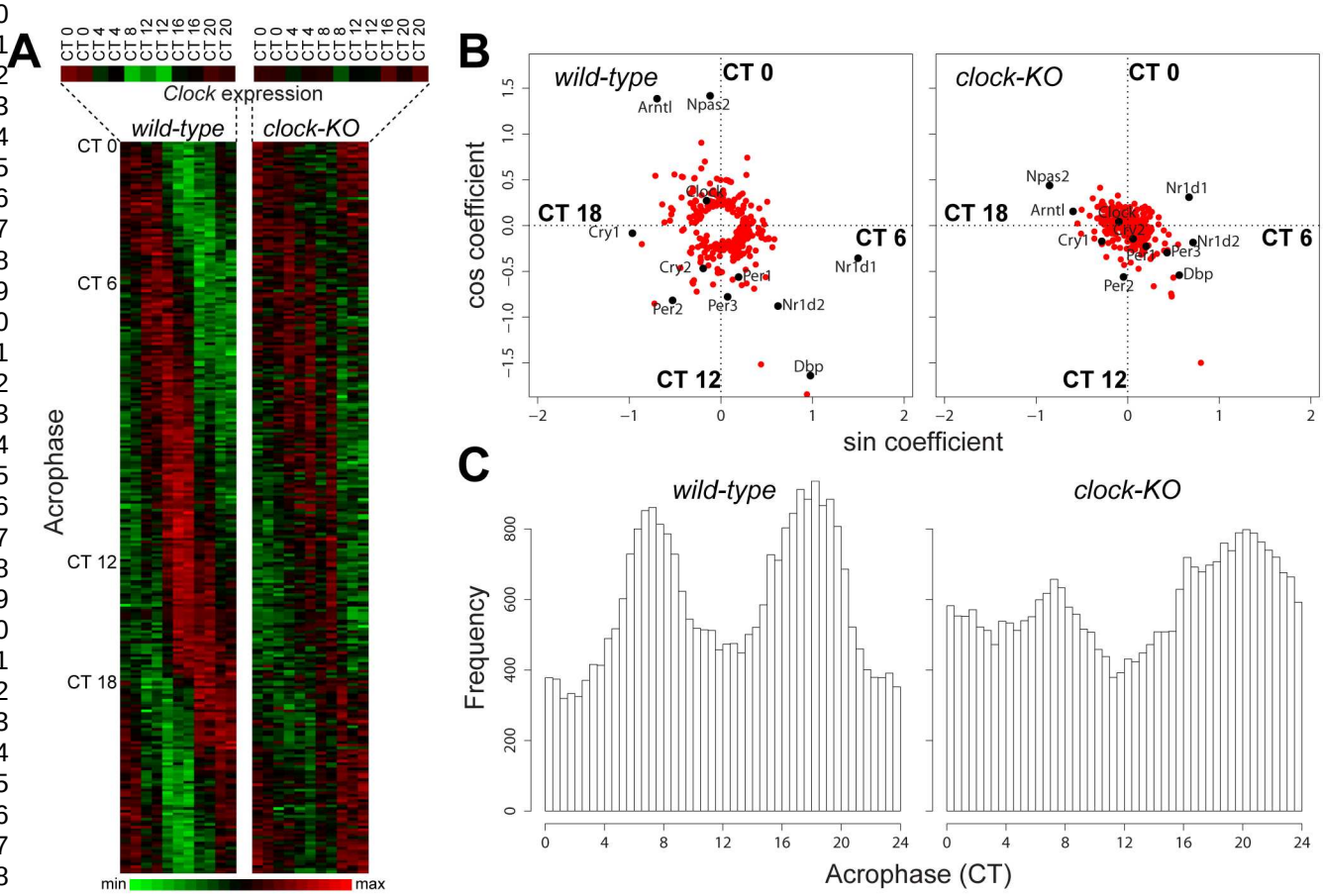

Nikolaeva et al., Figure 3

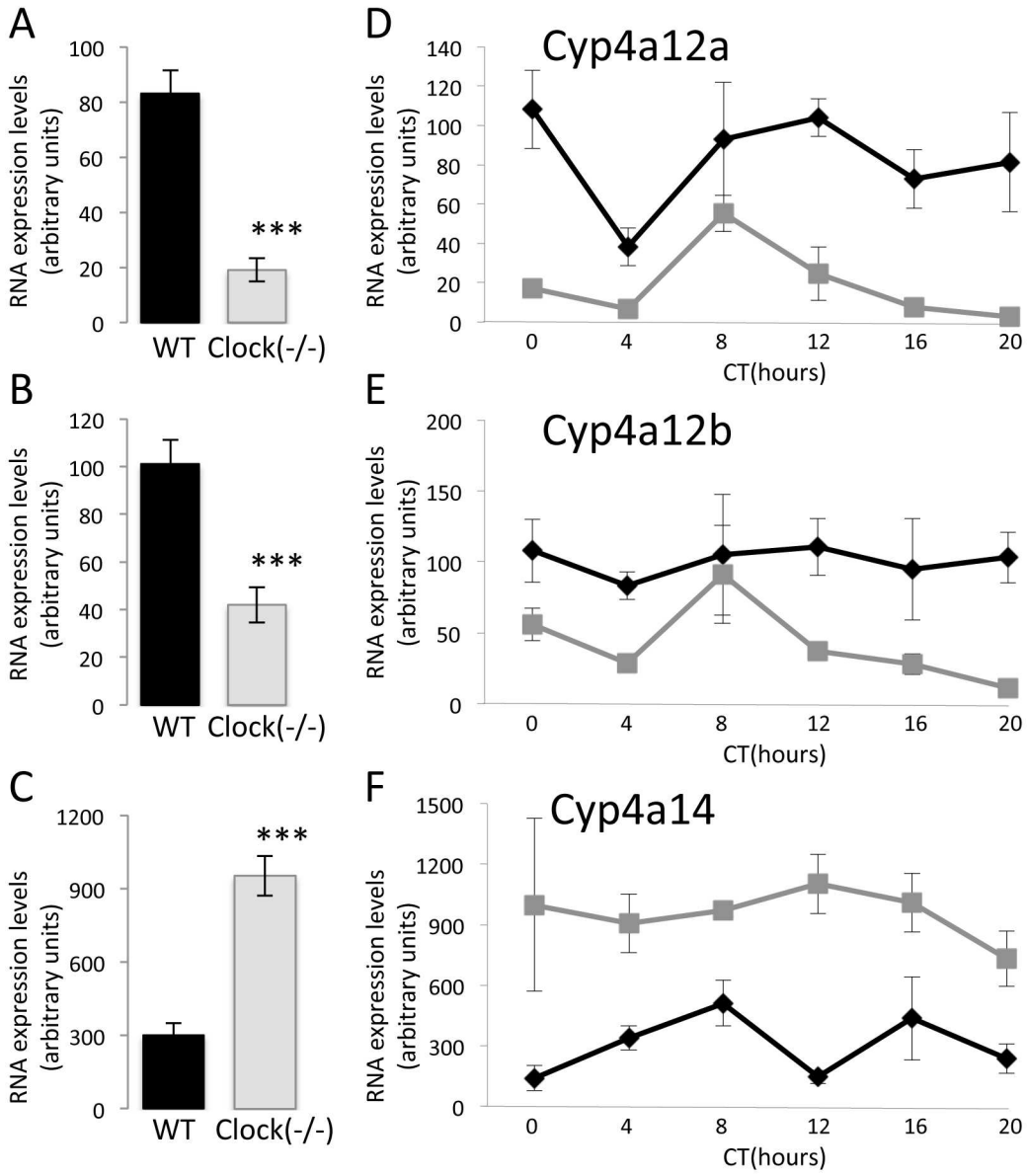

Nikolaeva et al., Figure 4

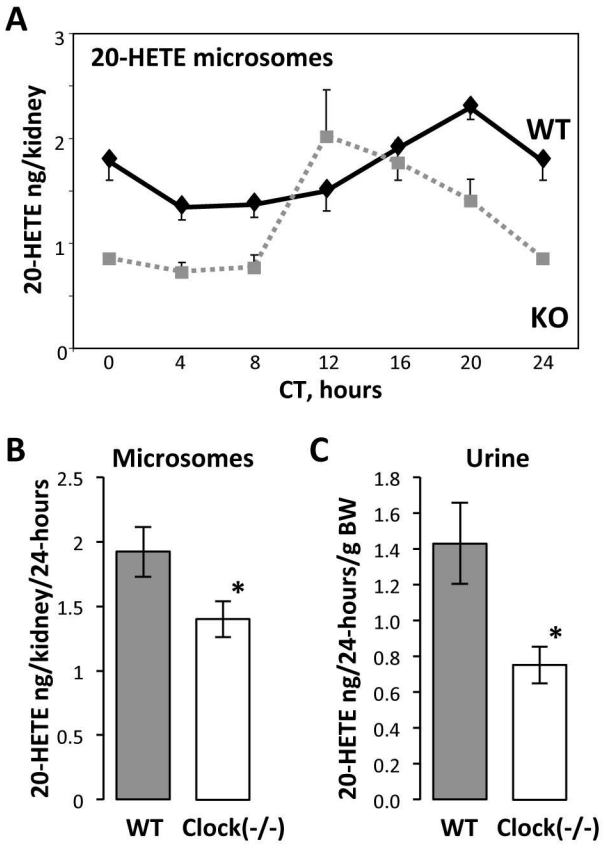

Nikolaeva et al., Figure 5

Table 1. Body weight, food and water intake and, sodium and potassium excretion rates in wild-type and *clock*-knockout mice.

	wild-type (n=11)	*clock*(-/-) (n=11)	
body weight (g) LD	25.82±0.19	26.14±0.26	NS
body weight (g) DD	25.90±0.42	25.90±0.56	NS
food intake (g/g body weight) LD	0.174±0.006	0.173±0.004	NS
food intake (g/g body weight) DD	0.189±0.004	0.195±0.003	NS
water intake (ml/g body weight) LD	0.193±0.009	0.209±0.009	NS
water intake (ml/g body weight) DD	0.197±0.006	0.239±0.011	p<0.005
UV*Na/g body weight (μmol/g) LD	5.67±0.39	7.67±0.44	p<0.005
UV*Na/g body weight (μmol/g) DD	5.74±0.46	7.18±0.72	NS
UK*K/g body weight (μmol/g) LD	24.75±1.50	27.35±1.41	NS
UV*K/g body weight (μmol/g) LD	23.22±1.46	26.45±1.19	NS

Supplementary methods

Microarrays expression profiling and data analysis RNA from whole kidneys of wild-type or *clock* deficient mice was isolated with the standard method of Chomczynski and Sacchi [1]. The RNA quality was assessed on the Agilent 2100 bioanalyzer chips. RNA extracted from 2 or 3 mice was pooled and 100 ng of the mix was used to perform target preparation using the Whole Transcript Sense Target Labeling Protocol procedure (Affymetrix, High Wycombe, UK). 5.5µg of each fragmented cDNA was end-labeled with biotin and hybridized to a Mouse Gene 1.0 ST array (Affymetrix), then processed and scanned according to standard procedures. Normalized expression signals were calculated from Affymetrix CEL files using RMA normalization method implemented in the Affymetrix Expression Console software. Microarray hybridization was performed on two biological replicates. Data have been deposited in NCBIs Gene Expression Omnibus (GEO, http://www.ncbi.nlm.nih.gov/geo/) and are accessible through GEO Series accession number GSE27366. All subsequent statistical analyses were performed using R (R Core, 2004, http://www.R-project.org) and Bioconductor packages (http://www.Bioconductor.org). Linear models were implemented using Limma package[2]. One WT ZT8 microarray and one KO ZT16 microarray that did not pass the quality controls were removed from subsequent analysis. To identify circadian genes, we applied separately to WT and KO samples the following linear model:

$$Y_i = \mu + \cos\theta + \sin\theta + \varepsilon_i$$

where Y_i is the log2 expression for the probe set i , and the time was decomposed in $\cos\theta$ and $\sin\theta$ sinusoidal pairs with the periodicity corresponding to 24 hours. θ was calculated as $2*\pi*t/\tau$, where t equals 0, 4, 8, 12, 16 or 20 h and τ is the period of 24 h. The sin and cos factors were combined into one F test. The P values from the F-test

for the WT and KO samples were adjusted together using the Benjamini and Hochberg's method to calculate the false discovery rate (FDR). Probe sets with a FDR < 0.1 were considered as significant. To identify genes differentially affected in WT and KO, we applied the following linear model:

$$Y_i = \mu + T_j + G_k + \varepsilon_i ,$$

where Y_i is the log2 expression for the probe set i at time T_j, in genotype condition (WT or KO) G_k. Specifically, μ (the intercept) estimated the mean expression for WT mice at ZT0. P values calculated for the genotype factor were adjusted for multiple testing and probe sets with a FDR < 0.1 and an absolute fold change > 50% were considered significant. Pathway enrichment analysis was performed using DAVID (http://david.abcc.ncifcrf.gov).

1. Chomczynski, P, Sacchi, N: Single-step method of RNA isolation by acid guanidinium thiocyanate-phenol-chloroform extraction. *Anal Biochem,* 162**:** 156-159., 1987.
2. Wettenhall, JM, Smyth, GK: limmaGUI: a graphical user interface for linear modeling of microarray data. *Bioinformatics,* 20**:** 3705-3706, 2004.

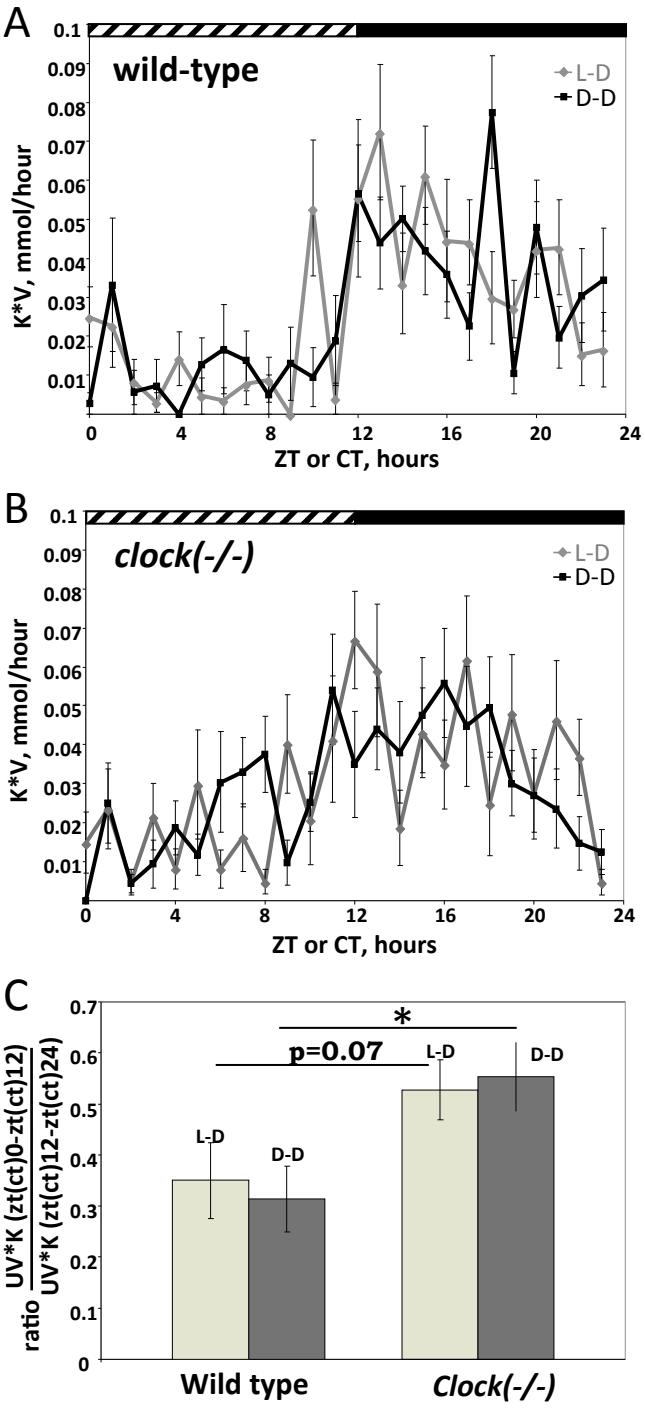

Supplementary Figure1. **A.** Temporal profile of renal potassium excretion rates in wild-type mice in LD or DD conditions. Values are averages ±SEM from n=11 mice. **B.** Temporal profile of renal potassium excretion rates in *clock(-/-)* mice in LD or DD conditions. Values are averages ±SEM from n=11 mice. **C.** Ratio between potassium excreted during the day (ZT0-ZT12) and the night (ZT12-ZT24) in LD conditions or during the subjective day (CT0-CT12) and subjective night (CT12-CT24) in DD conditions (*, $p<0.05$, n=11). Statistical significance was calculated using unpaired *t*-test.

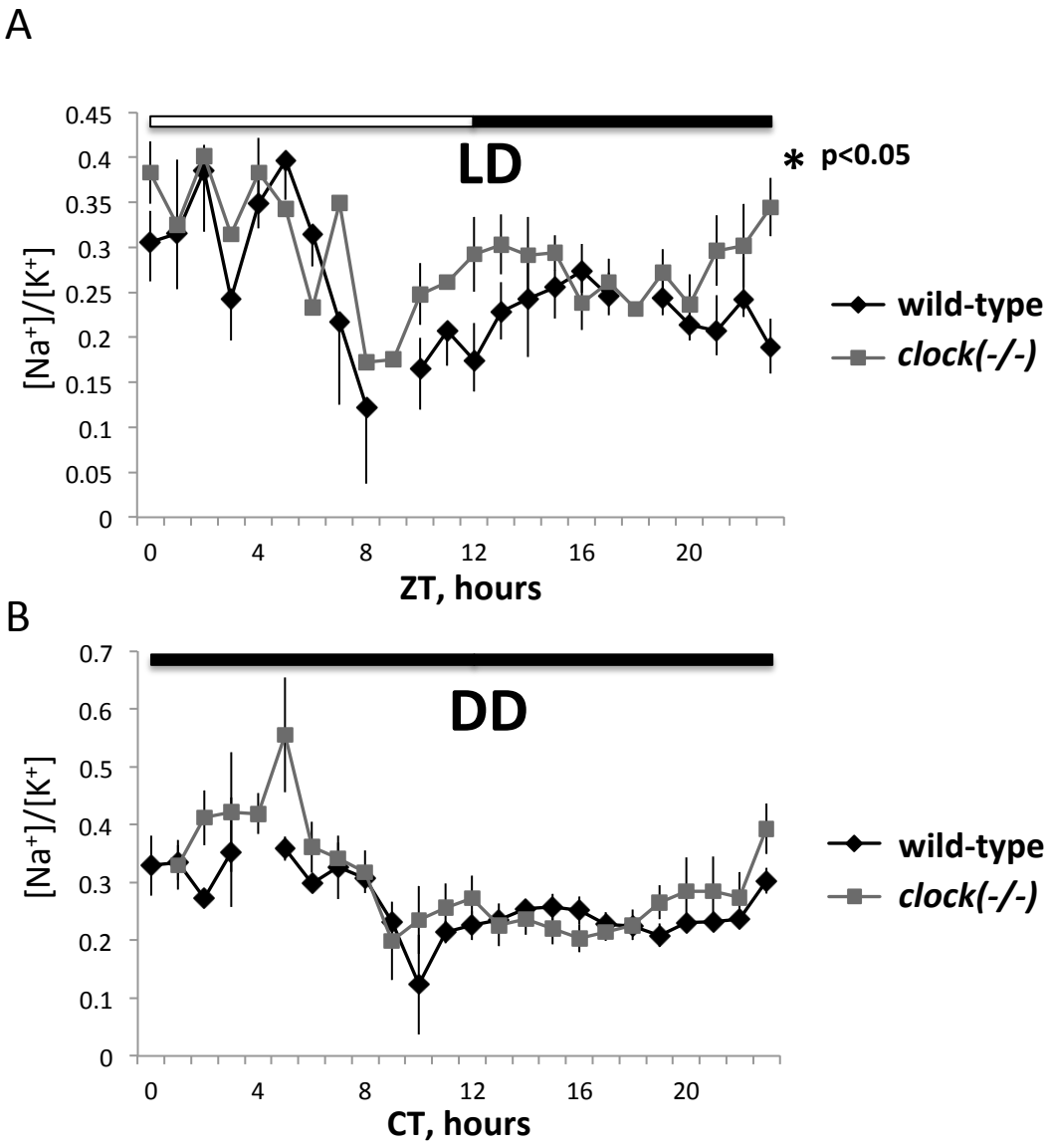

Supplementary Figure 2. **A.** Urinary Na^+/K^+ ratio in LD conditions. Values are averages ±SEM from n=11 mice. **B.** Urinary Na^+/K^+ ratio in DD conditions. Values are averages ±SEM from n=11 mice. Values for the Na^+/K^+ ratio at ZT9 (LD, wild-type mice), ZT4 (DD, wild-type mice) and ZT0 (DD, *clock(-/-)* mice) are missing because none of the animals examined (n=11) excreted detectable amounts of urine at these time-points.

Nikolaeva et al., Supplementary Figure 2

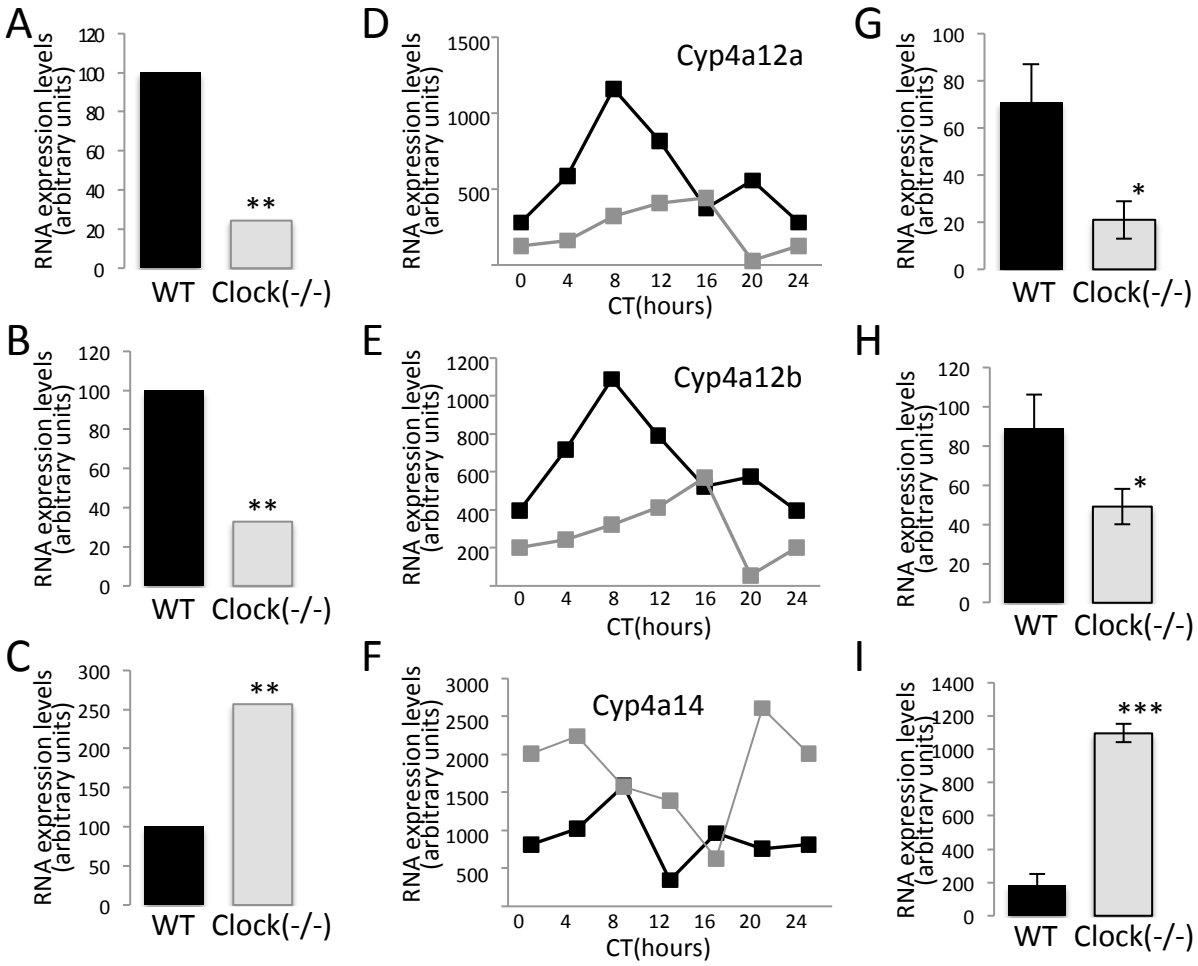

Supplementary Figure 3. Microarray analysis of Cyp4a12a, Cyp4a12b and Cyp4a14 RNA expression levels in kidneys of wild-type and *clock(-/-)* mice. Data presented in panels A, B and C are the 24-hour mean microarray hybridization signals for Cyp4a12a, Cyp4a12b and Cyp4a14, respectively. The RNA was extracted from whole kidneys of mice adapted to LD conditions for two weeks and then placed in constant darkness (DD) for 30 hours before sacrifice. Temporal expression profiles of Cyp4a12a, Cyp4a12b and Cyp4a14 in kidneys of wild-type (black line) and *clock(-/-)* (grey line) mice are shown in panels D, E and F, respectively. Data presented in panels D, E and F are means of microarray hybridization signals obtained from two biological replicates. Each biological replicate was composed of equimolar amounts of RNA extracted from 2 or 3 mice (see Supplementary Methods). Statistical analysis of microarray hybridization data was performed according to a standard protocol (see Supplementary Methods). ** - $p<0.01$. Data presented in panels G, H and I show qPCR-based quantitation of 24-hour mean Cyp4a12a, Cyp4a12b and Cyp4a14, expression levels in RNA samples extracted from the kidneys of mice maintained in the 12h:12k light-dark (LD) conditions. Values are means ±SEM from n=30 mice. Statistical significance was calculated using unpaired *t*-test. *, $p<0.05$; **, $p<0.01$; ***, $p<0.001$.

Supplementary Table 1. Circadian oscillatory transcripts in wild-type mice.

				Expression levels (A-values)					
Probe ID	**Symbol**	**FDR**	**Acrophase [CT]**	**CT 0**	**CT 4**	**CT 8**	**CT 12**	**CT 16**	**CT 20**
10345675	Npas2	0.0001	23.68	8.08	7.37	5.57	5.39	6.02	7.48
10494023	Rorc	0.0001	17.11	8.26	7.63	7.86	8.79	9.21	9.27
10390691	Nr1d1	0.0001	6.90	8.38	9.63	10.19	9.10	7.40	7.20
10356601	Per2	0.0001	14.19	6.61	6.53	7.35	8.27	8.24	7.48
10556463	Arntl	0.0001	22.22	8.44	7.47	5.58	5.64	7.32	8.28
10417734	Nr1d2	0.0002	9.64	8.20	9.25	9.87	9.95	9.06	7.99
10384378	Ddc	0.0003	1.78	10.03	10.01	9.56	8.90	9.01	9.55
10556266	Wee1	0.0005	12.50	7.85	8.05	8.70	9.16	8.81	8.23
10443332	Ppard	0.0014	22.74	8.29	7.83	7.13	7.08	7.55	8.18
10553092	Dbp	0.0019	9.95	7.07	8.54	10.83	10.55	8.28	7.50
10597960	Slc6a20a	0.0019	10.16	7.68	7.99	8.36	8.41	8.00	7.71
10558961	Tspan4	0.0019	12.21	8.56	8.66	9.32	9.58	9.24	8.81
10410530	Slc6a19	0.0019	7.06	10.61	11.07	11.31	10.95	10.27	10.29
10371400	Cry1	0.0019	17.67	6.91	5.77	5.91	7.02	7.58	7.49
10427095	Tenc1	0.0026	8.87	8.48	8.89	9.15	9.08	8.61	8.41
10349431	Acmsd	0.0026	23.97	10.61	10.48	10.02	9.63	9.98	10.50
10495035	Slc16a1	0.0026	23.11	9.95	9.58	8.45	8.11	9.08	9.73
10518781	Per3	0.0026	11.64	5.96	6.37	7.29	7.57	6.96	6.40
10389581	Ypel2	0.0026	21.42	7.75	7.12	6.54	6.66	7.36	7.80
10366707	Avpr1a	0.0026	23.07	8.87	8.43	7.92	7.38	8.12	8.73
10596454	Alas1	0.0026	13.93	10.58	10.47	10.89	11.39	11.24	10.90
10576901	Slc10a2	0.0026	22.08	9.76	9.31	8.81	8.66	9.35	9.73
10373452	Gm129	0.0027	10.20	5.03	6.07	8.39	8.89	6.11	5.06
10409278	Nfil3	0.0030	20.48	7.71	6.81	6.15	6.52	7.61	7.86
10496077	Agxt2l1	0.0040	9.22	6.60	7.15	7.66	7.47	6.91	6.56
10483000	Itgb6	0.0040	0.43	10.61	10.46	10.13	9.57	9.92	10.39
10363773	Rhobtb1	0.0047	21.19	9.33	8.59	8.04	8.00	9.11	9.24
10466304	Dtx4	0.0076	23.68	8.30	8.10	7.69	7.19	7.75	8.13
10574087	Herpud1	0.0076	13.17	11.18	11.28	11.73	11.82	11.86	11.48
10606989	Tsc22d3	0.0078	14.91	7.60	7.29	7.61	8.65	8.40	8.14
10542112	Clec2h	0.0081	6.97	8.97	9.63	9.72	9.35	8.70	8.65
10593225	Zbtb16	0.0112	13.34	6.84	6.70	7.28	8.29	7.87	7.14
10584634	Usp2	0.0112	12.30	9.22	9.40	9.99	10.19	9.91	9.57
10409162	Susd3	0.0116	13.16	6.98	6.99	7.40	7.90	7.62	7.28
10529671	Slc2a9	0.0117	9.76	7.60	8.03	8.33	8.28	7.95	7.65
10538658	Herc3	0.0117	7.53	8.62	9.25	9.35	9.20	8.41	8.31
10539933	Txnrd3	0.0117	5.72	7.65	7.97	7.90	7.64	7.37	7.41
10479047	Pck1	0.0121	15.12	12.10	11.99	12.23	12.54	12.70	12.39
10472923	Ak3l1	0.0121	14.17	10.51	10.44	10.83	11.22	11.15	10.88
10586368	Clpx	0.0121	0.34	10.43	10.29	9.90	9.79	9.84	10.27
10363224	Fabp7	0.0121	1.41	7.35	7.17	6.51	5.83	5.97	6.69
10471586	Hspa5	0.0121	18.85	11.64	11.36	11.08	11.36	12.21	12.11
10394735	Pdia6	0.0121	20.97	10.88	10.57	10.40	10.29	10.82	11.03
10425601	Tef	0.0123	11.18	8.69	9.09	9.67	9.95	9.38	8.94
10498978	Lrat	0.0123	2.27	5.89	6.03	5.54	5.28	5.18	5.61
10587639	Nt5e	0.0133	21.07	10.06	9.69	9.20	9.28	10.00	10.09
10404250	Dcdc2a	0.0133	0.71	6.99	7.01	6.35	6.04	6.35	6.73
10487879	Rnf24	0.0134	10.72	7.86	8.31	8.99	9.27	8.47	8.06
10502240	Npnt	0.0149	23.03	9.88	9.67	9.13	8.90	9.49	9.73
10504582	1300002K09Rik	0.0149	1.83	7.56	7.63	7.36	7.04	7.05	7.42
10472199	Upp2	0.0150	10.15	7.21	7.53	8.12	8.65	7.53	6.97
10381006	Thra	0.0157	3.03	8.58	8.74	8.45	8.05	7.99	8.25
10578207	Lonrf1	0.0157	12.26	6.65	6.64	7.25	7.61	7.29	6.73
10545874	Cml5	0.0158	14.69	8.20	7.89	8.43	10.12	9.78	9.21
10539295	Dqx1	0.0170	6.90	6.22	6.45	6.58	6.37	5.99	5.95
10476314	Prnp	0.0170	13.53	9.86	9.86	10.17	10.55	10.49	10.09
10469867	Pnpla7	0.0183	8.91	7.67	7.84	8.16	8.10	7.67	7.49
10485170	Cry2	0.0185	13.49	6.98	7.16	7.78	8.04	7.85	7.70
10414269	Bnip3	0.0189	11.77	10.12	10.28	10.50	10.67	10.50	10.24
10584712	Hyou1	0.0189	19.30	9.63	9.38	9.12	9.21	10.16	10.18
10350806	Nphs2	0.0200	2.15	9.58	9.55	9.38	8.87	8.90	9.24
10506269	Ak3l1	0.0202	13.99	9.47	9.48	9.84	10.28	10.18	9.90
10416689	Olfm4	0.0212	9.60	7.67	7.99	8.22	8.38	7.81	7.69
10530733	Clock	0.0213	21.99	9.13	8.86	8.49	8.55	8.90	9.03
10550956	Ethe1	0.0225	0.62	8.81	8.68	8.26	7.80	8.08	8.55
10346298	Coq10b	0.0229	11.92	8.81	8.83	9.41	9.76	9.38	8.83
10517744	Arhgef10l	0.0233	23.56	8.91	8.77	8.46	8.27	8.47	8.88
10472820	Itga6	0.0239	22.04	9.88	9.67	8.84	8.86	9.65	9.93

10556553	Insc	0.0251	20.43	6.47	6.09	5.79	5.95	6.46	6.59
10438769	Cldn1	0.0256	0.87	8.07	7.90	7.48	7.11	7.24	7.74
10349711	Slc41a1	0.0259	6.71	7.53	7.70	7.80	7.63	7.30	7.30
10587211	Leo1	0.0275	21.84	7.08	6.74	6.15	6.48	6.71	7.02
10438340	Comt1	0.0276	23.94	11.34	11.27	11.07	10.77	10.99	11.31
10429140	Ndrg1	0.0276	22.81	13.00	12.92	12.42	12.27	12.79	12.96
10581036	Tk2	0.0278	7.19	7.03	7.42	7.47	7.34	6.85	6.88
10371482	Hsp90b1	0.0279	20.34	11.81	11.65	11.25	11.41	11.94	12.02
10549473	Caprin2	0.0295	5.74	6.60	6.78	6.85	6.50	6.22	6.21
10377439	Per1	0.0296	10.73	6.88	7.66	7.69	8.32	7.57	7.28
10558921	Pnpla2	0.0301	8.44	8.45	8.77	8.90	8.79	8.55	8.32
10408251	Slc17a4	0.0304	6.24	5.49	6.03	5.86	5.64	5.25	5.27
10445241	Tnfrsf21	0.0304	12.13	10.50	10.59	10.81	11.19	10.92	10.58
10422009	---	0.0304	20.36	5.19	4.65	4.50	4.69	4.97	5.62
10454369	Fhod3	0.0304	5.81	7.58	7.92	7.92	7.54	7.39	7.38
10481634	Slc25a25	0.0306	15.48	9.19	9.18	9.22	9.62	10.02	9.51
10366712	Ppm1h	0.0339	23.21	8.72	8.64	8.10	7.93	8.41	8.62
10500272	Gm129	0.0339	10.93	4.77	5.28	7.80	8.06	5.78	5.53
10503502	Ttpa	0.0340	10.05	5.54	5.97	6.29	6.53	5.96	5.45
10382271	Arsg	0.0341	4.40	8.61	8.78	8.78	8.30	7.81	8.25
10596575	Manf	0.0341	18.37	8.41	8.20	7.91	8.24	9.17	8.90
10374453	Glul	0.0341	15.00	11.64	11.53	11.69	11.95	12.05	11.78
10350800	Tor1aip2	0.0341	6.95	8.27	8.63	8.66	8.48	8.12	8.11
10603125	Asb9	0.0341	3.77	8.35	8.31	8.29	7.91	7.52	7.89
10381445	Tmem106a	0.0341	8.51	9.00	9.33	9.41	9.42	9.05	8.91
10482846	Ccdc148	0.0341	8.39	5.62	6.12	6.10	6.29	5.62	5.41
10460157	Cpt1a	0.0341	8.39	10.98	11.17	11.40	11.31	10.94	10.85
10537410	Tbxas1	0.0351	3.52	7.12	7.31	7.13	6.78	6.67	6.92
10441038	Hlcs	0.0372	6.38	6.20	6.50	6.49	6.29	6.05	6.06
10405576	Fbxl21	0.0379	6.81	6.11	6.35	6.58	6.28	5.73	5.76
10435733	Igsf11	0.0389	1.16	9.69	9.70	9.47	9.11	9.33	9.52
10386473	Srebf1	0.0427	18.96	8.33	8.15	7.98	8.16	8.65	8.67
10406941	Sgtb	0.0429	7.11	5.69	6.23	6.25	6.00	5.56	5.42
10438098	Sdf2l1	0.0461	19.32	7.85	7.47	7.33	7.28	8.45	8.46
10519488	Tubb2c	0.0461	19.90	10.37	10.17	10.04	10.14	10.43	10.57
10545865	Cml3	0.0482	13.74	10.19	10.01	10.57	11.43	11.08	10.58
10426098	Creld2	0.0485	18.21	8.30	8.09	7.95	8.13	9.22	8.92
10438639	Dgkg	0.0490	4.20	7.02	7.60	7.16	6.75	6.22	6.83
10444459	Tnxb	0.0490	12.16	6.69	6.88	7.05	7.28	7.11	6.88
10421309	Slc39a14	0.0492	10.56	7.84	7.97	8.21	8.40	8.04	7.80
10395259	Nampt	0.0492	13.10	9.73	9.73	9.98	10.32	10.19	9.86
10515220	Faah	0.0508	2.12	8.73	8.73	8.64	8.28	8.33	8.54
10480628	Tubb2c	0.0508	19.84	10.38	10.21	10.07	10.16	10.47	10.58
10548194	Fkbp4	0.0509	20.66	10.11	9.95	9.65	9.75	10.15	10.18
10549222	Bcat1	0.0512	6.82	8.92	9.06	9.34	9.08	8.43	8.43
10484207	2610301F02Rik	0.0512	21.39	8.33	7.95	7.54	7.50	8.18	8.35
10545862	Cml3	0.0512	13.78	10.29	10.05	10.66	11.55	11.20	10.65
10417759	Ube2e2	0.0512	6.25	7.77	8.11	8.06	7.90	7.54	7.65
10601312	Gm10454	0.0512	23.92	8.34	8.10	7.76	7.62	7.84	8.06
10364287	Sumo3	0.0512	1.55	8.84	8.89	8.61	8.43	8.42	8.74
10546056	Rab43	0.0520	10.07	6.90	7.18	7.41	7.41	7.14	7.00
10444578	Neu1	0.0523	6.09	10.13	10.33	10.38	10.18	9.87	9.98
10486833	Ell3	0.0538	7.13	6.49	6.70	6.86	6.87	5.92	6.01
10406176	Slc9a3	0.0538	7.52	10.03	10.24	10.39	10.15	10.01	9.80
10369379	Slc29a3	0.0543	3.92	9.32	9.40	9.24	9.06	8.85	9.02
10479979	Slc25a36	0.0549	6.93	9.87	10.28	10.33	10.04	9.80	9.73
10468762	4930506M07Rik	0.0550	3.24	7.31	7.54	7.06	7.01	6.75	7.08
10438530	Clcn2	0.0550	10.92	7.29	7.48	7.74	7.83	7.55	7.42
10545869	Cml3	0.0551	13.70	10.21	9.96	10.59	11.47	11.12	10.54
10444895	Flot1	0.0553	8.14	7.20	7.41	7.68	7.52	7.13	7.06
10480090	Itga8	0.0558	5.53	8.01	8.15	8.10	7.83	7.37	7.34
10402195	Tc2n	0.0558	9.27	6.24	6.98	7.28	7.60	6.46	6.22
10517036	Wdtc1	0.0560	2.81	8.62	8.71	8.50	8.36	8.31	8.46
10360684	Ephx1	0.0565	10.22	9.16	9.38	9.61	9.78	9.44	9.04
10422013	Klf12	0.0572	7.89	7.65	7.80	7.96	7.93	7.48	7.39
10580219	Calr	0.0577	21.73	11.56	11.40	11.08	11.09	11.48	11.54
10556487	A630005I04Rik	0.0592	21.46	6.44	5.46	4.97	5.37	5.67	6.26
10521759	Slit2	0.0592	8.67	8.30	8.46	8.68	8.65	8.28	8.10
10534281	Clip2	0.0592	2.05	7.70	7.78	7.52	7.27	7.39	7.49
10362201	Ctgf	0.0597	12.81	9.75	9.78	10.03	10.28	10.12	9.90
10373740	Pik3ip1	0.0648	10.92	6.50	6.69	7.02	6.95	6.78	6.66
10542200	Gabarapl1	0.0649	6.15	11.32	11.53	11.52	11.33	11.11	11.08

10425987	Ppara	0.0655	9.56	8.93	9.14	9.32	9.37	9.04	8.94
10556701	Acsm5	0.0655	8.57	9.13	9.41	9.72	9.65	9.09	8.96
10523758	Lrrc8b	0.0655	7.26	8.24	8.49	8.48	8.41	8.16	8.03
10449741	Sik1	0.0655	13.68	9.21	9.24	9.42	9.74	9.60	9.47
10521626	Cc2d2a	0.0673	4.87	7.33	7.58	7.39	7.25	6.95	7.13
10593384	Dixdc1	0.0673	5.46	6.70	6.88	6.79	6.67	6.39	6.47
10464754	Rhod	0.0673	3.88	7.87	8.07	7.94	7.58	7.61	7.66
10483157	---	0.0675	20.21	4.79	4.39	4.39	4.30	4.81	4.92
10510516	Slc2a5	0.0676	9.63	9.20	9.34	9.73	9.66	9.26	9.22
10364237	Gm10787	0.0690	15.29	6.34	6.20	6.61	7.04	6.96	6.99
10559790	Zim1	0.0690	2.12	5.44	5.29	5.06	4.79	4.66	5.01
10439976	2310061J03Rik	0.0692	7.74	5.92	6.15	6.37	6.26	5.73	5.77
10539342	Rtkn	0.0704	14.97	6.65	6.63	6.83	7.15	7.14	7.05
10361250	Camk1g	0.0730	0.07	6.42	6.39	5.78	5.75	5.99	6.23
10527475	Zfp655	0.0732	9.06	7.76	8.04	8.20	8.22	7.86	7.72
10501302	Sypl2	0.0732	15.02	8.08	7.93	8.08	8.48	8.39	8.28
10344952	Rdh10	0.0732	22.88	10.57	10.47	10.13	9.82	10.36	10.57
10485282	Alkbh3	0.0732	8.36	8.68	8.85	8.98	8.93	8.67	8.57
10362073	Sgk1	0.0732	17.49	8.71	8.29	8.21	8.77	9.13	8.90
10553324	Tmem86a	0.0736	5.90	8.20	8.73	8.84	8.38	7.69	8.18
10379044	Rab34	0.0738	9.46	8.30	8.49	8.70	8.71	8.39	8.28
10378848	Hsp90aa1	0.0738	20.03	12.13	11.96	11.65	11.79	12.29	12.27
10440238	Nsun3	0.0738	7.46	7.85	8.18	8.22	8.16	7.71	7.67
10468802	D19Ertd737e	0.0742	7.15	7.16	7.48	7.39	7.37	7.06	6.97
10362314	Ptprk	0.0756	0.99	10.00	10.01	9.81	9.49	9.70	9.87
10421293	Ppp3cc	0.0757	8.85	7.62	7.83	8.02	8.03	7.64	7.54
10484201	2610301F02Rik	0.0757	21.27	9.03	8.67	8.20	8.18	8.98	9.01
10549276	Bhlhe41	0.0757	10.40	5.00	5.24	6.39	6.29	5.35	5.16
10568785	Bnip3	0.0757	11.91	9.21	9.39	9.69	9.79	9.56	9.48
10431147	Ldoc1l	0.0757	23.14	7.18	7.02	6.81	6.51	6.69	7.36
10399478	Lpin1	0.0757	10.60	9.10	9.45	9.67	9.96	9.39	9.33
10539632	Alms1	0.0757	10.65	5.00	5.14	5.45	5.83	5.21	4.96
10544906	Ggct	0.0757	3.17	7.54	7.54	7.43	7.20	7.04	7.26
10489620	Ncoa5	0.0757	20.89	8.08	7.89	7.62	7.77	8.02	8.11
10441270	Ripk4	0.0757	11.58	7.33	7.66	7.72	7.90	7.83	7.49
10399874	Bcap29	0.0763	7.70	8.14	8.36	8.44	8.35	8.08	7.99
10485117	Creb3l1	0.0765	0.19	6.79	6.74	6.40	6.22	6.47	6.64
10356406	Ngef	0.0765	11.97	8.14	8.29	8.42	8.59	8.47	8.26
10463211	Pi4k2a	0.0765	22.50	9.06	9.00	8.66	8.53	8.91	9.12
10348451	Cxcr7	0.0765	20.96	7.60	7.26	6.73	7.16	7.37	7.69
10484197	2610301F02Rik	0.0774	21.52	8.09	7.83	7.14	7.24	8.00	8.09
10354563	Dnahc7b	0.0775	6.68	6.12	6.60	6.34	6.29	6.06	5.90
10378453	1300001I01Rik	0.0775	0.55	10.75	10.68	10.51	10.26	10.42	10.62
10539640	Alms1	0.0775	10.74	4.90	5.05	5.31	5.74	5.14	4.86
10358454	Rbm3	0.0775	10.30	10.20	10.67	10.92	10.94	10.62	10.44
10499483	Fdps	0.0775	22.25	8.06	7.98	7.71	7.55	7.94	8.16
10454235	Asxl3	0.0775	23.12	6.55	6.42	6.23	6.17	6.24	6.58
10557843	Fus	0.0784	6.48	9.02	9.45	9.20	9.30	8.56	8.65
10373902	Gatsl3	0.0784	9.11	7.13	7.51	7.77	7.94	7.16	7.08
10491780	Hspa4l	0.0784	19.80	8.74	8.59	8.34	8.48	8.91	8.94
10525893	Aacs	0.0790	15.13	9.85	9.65	10.20	10.54	10.44	10.46
10510270	Mthfr	0.0790	22.68	7.85	7.68	7.18	7.42	7.50	7.77
10505187	Ugcg	0.0798	7.77	7.10	7.53	7.51	7.42	7.14	7.07
10402615	Hsp90aa1	0.0802	19.92	11.75	11.61	11.30	11.44	11.95	11.91
10419779	Haus4	0.0804	6.32	6.70	6.86	7.08	6.75	6.43	6.56
10408928	Hspb1	0.0810	18.41	7.81	7.58	7.68	7.67	8.11	8.05
10394942	Taf1b	0.0810	6.07	7.02	7.32	7.31	7.10	6.74	6.86
10574350	Mmp15	0.0810	22.86	6.53	6.36	6.06	6.07	6.18	6.54
10417579	4930452B06Rik	0.0810	7.61	5.16	5.31	5.51	5.37	5.01	5.00
10558150	Htra1	0.0810	1.58	9.75	9.87	9.55	9.36	9.50	9.63
10455259	Arhgap26	0.0810	1.81	8.33	8.38	7.99	7.83	7.86	8.09
10518532	Tardbp	0.0810	18.70	9.23	9.06	8.81	9.19	9.41	9.45
10452815	Xdh	0.0810	10.93	7.74	7.92	8.08	8.19	7.99	7.82
10603208	Mid1	0.0810	0.90	7.82	7.88	7.48	7.38	7.54	7.67
10433597	Snx29	0.0810	23.66	10.36	10.19	9.92	9.84	10.00	10.21
10419240	Ddhd1	0.0810	22.75	8.70	8.50	8.27	8.21	8.42	8.62
10498871	Tmem144	0.0810	5.51	8.80	8.88	8.99	8.71	8.23	8.40
10359118	Tdrd5	0.0810	0.56	6.26	6.09	6.13	5.75	5.84	6.17
10419854	Slc7a8	0.0810	23.78	11.13	11.03	10.74	10.61	10.78	11.05
10526410	Hspb1	0.0810	18.41	7.78	7.47	7.55	7.61	8.08	7.98
10517312	Tmem57	0.0821	12.94	8.21	8.14	8.38	8.61	8.43	8.28
10401488	Abcd4	0.0821	7.12	8.02	8.16	8.31	8.19	7.79	7.83

10480035	Pfkfb3	0.0841	9.78	7.27	7.64	7.65	7.90	7.51	7.27
10377560	Sat2	0.0846	7.35	7.98	8.18	8.35	8.19	7.83	7.88
10603469	Rbm3	0.0849	10.31	9.97	10.41	10.66	10.69	10.37	10.19
10390103	Pdk2	0.0849	7.90	10.47	10.69	10.81	10.69	10.46	10.39
10535904	Hsph1	0.0849	17.60	10.31	9.95	9.81	10.26	10.83	10.40
10607585	Gm15190	0.0849	19.67	6.19	6.01	5.84	6.01	6.25	6.35
10428012	Ropn1l	0.0859	8.79	6.09	6.31	6.41	6.47	6.10	6.05
10479902	Dhtkd1	0.0859	9.45	8.26	8.52	8.63	8.82	8.37	8.18
10358177	5730559C18Rik	0.0859	19.70	7.18	7.06	6.75	7.02	7.29	7.36
10409240	Sema4d	0.0859	6.45	8.55	8.80	8.73	8.58	8.49	8.35
10401935	BC005685	0.0874	12.85	3.92	3.99	4.33	4.40	4.30	4.17
10497682	Kcnmb3	0.0874	19.18	6.34	6.16	6.04	6.20	6.48	6.52
10395039	Cmpk2	0.0874	20.89	7.16	6.93	6.78	6.70	7.15	7.29
10565456	Prss23	0.0874	0.91	7.55	7.61	7.33	7.02	7.27	7.44
10504757	BC005685	0.0880	11.88	4.25	4.28	4.68	4.73	4.49	4.40
10425999	Ttc38	0.0893	9.32	8.75	8.98	9.08	9.14	8.89	8.66
10405693	Dapk1	0.0908	23.16	9.58	9.51	9.28	9.11	9.42	9.53
10492522	Schip1	0.0908	21.49	8.01	7.72	7.61	7.64	7.79	8.01
10370665	Med16	0.0908	7.05	8.00	8.28	8.27	8.11	7.99	7.90
10491915	Ccrn4l	0.0908	14.44	7.44	7.51	7.58	7.88	8.05	7.67
10417869	Anxa7	0.0908	10.60	8.03	8.24	8.47	8.47	8.26	8.18
10485013	1110051M20Rik	0.0926	7.99	7.68	7.86	7.95	7.91	7.63	7.57
10569545	Nadsyn1	0.0926	10.09	7.60	7.77	7.93	8.03	7.74	7.61
10411456	Tmem174	0.0931	7.75	11.08	11.28	11.52	11.37	10.93	11.02
10428857	Mtss1	0.0934	9.96	8.76	8.83	9.21	9.19	8.82	8.74
10467768	Loxl4	0.0934	0.32	6.65	6.58	6.08	6.11	6.17	6.47
10571364	1700016D18Rik	0.0934	7.66	3.32	3.51	3.77	3.53	3.23	3.15
10593526	Atm	0.0934	6.08	7.59	7.71	7.71	7.62	7.21	7.28
10508707	Tmem200b	0.0934	14.91	7.19	7.09	7.30	7.52	7.54	7.39
10500555	Hsd3b3	0.0944	14.01	9.00	8.93	9.00	9.58	9.38	9.16
10570280	F7	0.0944	15.60	5.15	5.01	5.10	5.36	5.40	5.26
10496373	Ddit4l	0.0952	23.46	7.85	7.42	7.18	7.00	7.36	7.39
10453057	Cyp1b1	0.0953	4.91	8.33	8.69	8.64	8.09	8.08	8.07
10406598	Serinc5	0.0953	5.18	8.13	8.28	8.32	8.01	7.74	7.88
10403312	Akr1c19	0.0958	14.07	7.81	7.82	7.92	8.48	8.35	8.09
10385540	Olfr1396	0.0959	22.48	6.19	5.91	5.69	5.76	5.87	6.05
10500362	Polr3gl	0.0960	10.27	8.16	8.33	8.45	8.54	8.32	8.18
10532150	Fam69a	0.0967	4.96	8.76	8.89	8.94	8.64	8.38	8.57
10599192	Lonrf3	0.0967	19.19	7.47	6.48	6.73	6.92	7.44	7.50
10587829	Plod2	0.0967	0.24	8.94	9.05	8.35	8.26	8.54	8.85
10389786	Hlf	0.0967	14.03	8.70	8.79	9.04	9.28	9.21	9.12
10544837	1200009O22Rik	0.0967	23.72	7.30	7.13	7.07	6.71	6.92	7.26
10399680	Cys1	0.0967	13.15	7.05	7.10	7.11	7.48	7.40	7.10
10400748	Cdkl1	0.0968	0.01	10.63	10.42	10.20	10.12	10.16	10.47
10385872	Slc22a5	0.0973	11.58	9.83	9.89	10.12	10.14	10.05	9.87
10499378	Sema4a	0.0973	3.93	9.70	9.82	9.79	9.49	9.41	9.55
10451079	4930564C03Rik	0.0973	15.46	5.13	4.96	5.19	5.42	5.48	5.34
10481435	Ccbl1	0.0975	9.43	9.48	9.74	10.04	10.21	9.51	9.46
10513587	Rnf183	0.0976	0.20	9.14	9.09	8.93	8.67	8.87	9.07
10526559	Ache	0.0976	10.29	5.75	5.83	6.15	6.11	6.03	5.52
10596318	Nudt16	0.0976	8.82	6.58	6.93	7.14	7.02	6.71	6.57
10468159	Ldb1	0.0976	7.53	8.75	8.92	8.98	8.91	8.68	8.64
10545886	1700019G17Rik	0.0976	5.83	6.74	6.91	6.95	6.69	6.41	6.43
10440091	Col8a1	0.0976	0.57	6.99	7.03	6.70	6.51	6.73	6.89
10565727	Tsku	0.0977	12.85	6.98	6.99	7.42	7.84	7.37	7.34
10385822	Gm10447	0.0977	15.91	4.48	4.39	4.62	4.83	4.86	4.91
10481845	Fam125b	0.0978	6.09	7.33	7.48	7.53	7.35	7.09	7.13
10365658	Uhrf1bp1l	0.0979	9.03	8.87	9.04	9.12	9.18	8.92	8.75
10364712	Cirbp	0.0979	6.99	8.37	8.94	9.41	8.81	8.01	8.41
10395394	4930579E17Rik	0.0987	7.16	5.87	6.07	6.08	6.03	5.70	5.59
10422312	Cldn10	0.0987	1.56	11.01	11.02	10.85	10.69	10.66	10.93
10565794	Serpinh1	0.0989	19.63	7.70	7.36	7.29	7.41	7.75	7.78
10544525	Pdia4	0.0989	19.26	10.24	10.14	9.94	10.00	10.59	10.50
10458285	5133400G04Rik	0.0989	8.20	6.03	6.37	6.35	6.42	6.02	6.01
10420889	1110020C17Rik	0.0998	16.93	4.02	3.81	4.05	4.08	4.45	4.27

Supplementary Table 2. Circadian oscillatory transcripts in *clock*-knockout mice.

				Expression levels (A-values)					
Probe ID	**Symbol**	**FDR**	**Acrophase [CT]**	**CT 0**	**CT 4**	**CT 8**	**CT 12**	**CT 16**	**CT 20**
10345675	Npas2	0.0024	19.81	7.87	7.08	6.36	6.93	5.98	8.21
10443332	Ppard	0.0026	19.26	7.83	7.39	7.20	7.47	7.41	8.23
10463355	Scd2	0.0040	17.90	9.98	9.52	9.61	9.97	10.07	10.25
10602372	Alas2	0.0047	4.25	7.11	7.50	7.12	6.69	7.21	6.54
10476314	Prnp	0.0079	9.40	9.60	9.86	10.22	10.19	10.63	9.33
10545869	Cml3	0.0123	9.88	9.29	9.49	10.39	10.68	11.11	8.62
10496077	Agxt2l1	0.0123	8.10	6.88	7.22	7.61	7.37	6.92	6.54
10506269	Ak3l1	0.0154	10.84	9.43	9.64	9.87	9.95	10.24	9.46
10403303	Akr1c13	0.0157	7.83	6.96	7.18	7.54	7.27	6.58	6.64
10349431	Acmsd	0.0160	21.59	10.61	10.30	9.72	9.84	9.99	10.71
10364712	Cirbp	0.0170	5.00	8.68	9.07	8.89	8.53	8.24	8.42
10392522	Abca8a	0.0170	11.69	7.55	7.82	8.08	8.27	8.56	7.73
10545865	Cml3	0.0170	9.84	9.35	9.50	10.38	10.66	11.10	8.64
10366712	Ppm1h	0.0171	20.37	8.74	8.57	8.34	8.43	8.38	8.89
10545862	Cml3	0.0182	9.86	9.43	9.55	10.49	10.77	11.21	8.68
10450038	Angptl4	0.0188	7.27	7.32	7.82	7.88	7.62	7.85	6.92
10492306	Sucnr1	0.0189	7.20	9.02	9.19	9.42	9.14	9.15	8.51
10434675	Dnajb11	0.0195	17.99	9.58	9.37	9.32	9.59	9.97	9.84
10356601	Per2	0.0202	12.30	6.68	7.03	7.53	7.91	8.17	7.15
10549025	Slco1a6	0.0207	8.54	10.07	10.39	10.50	10.56	10.83	9.67
10459879	Slc14a2	0.0213	20.01	7.80	7.58	7.49	7.55	7.54	8.09
10375051	Hba-a1	0.0213	3.96	12.23	12.51	12.20	11.82	12.29	11.82
10375058	Hba-a2	0.0220	3.98	12.13	12.42	12.11	11.73	12.23	11.71
10378568	---	0.0239	8.79	6.79	6.94	7.18	7.22	6.90	6.43
10435075	Tfrc	0.0251	18.76	10.20	9.79	9.68	10.01	10.31	10.25
10580219	Calr	0.0251	19.18	11.41	11.25	11.07	11.26	11.53	11.64
10467766	Loxl4	0.0251	19.63	5.83	5.29	5.20	5.16	5.19	6.68
10429856	Spatc1	0.0253	7.72	6.39	6.61	7.02	6.71	6.73	6.11
10408656	Peci	0.0253	9.25	9.33	9.55	9.75	9.74	9.72	9.20
10472820	Itga6	0.0256	18.96	10.02	9.68	9.55	9.80	9.69	10.37
10438098	Sdf2l1	0.0275	18.15	7.70	7.42	7.08	7.75	8.39	8.14
10526232	Wbscr27	0.0276	5.43	7.43	7.61	7.58	7.38	7.18	7.19
10479902	Dhtkd1	0.0289	7.71	8.34	8.64	8.94	8.65	8.42	7.96
10483000	Itgb6	0.0304	21.67	10.65	10.47	10.22	10.12	9.98	10.75
10545874	Cml5	0.0304	10.13	5.62	5.93	7.61	8.58	10.09	4.67
10519951	Pion	0.0304	7.51	7.03	7.40	7.42	7.43	7.34	6.80
10373374	Slc39a5	0.0304	21.52	9.14	8.96	8.61	8.71	8.77	9.27
10496813	Ctbs	0.0305	7.24	8.48	8.70	8.82	8.62	8.51	8.25
10353450	Gm4956	0.0305	10.93	5.27	5.49	6.06	6.26	6.59	5.30
10502240	Npnt	0.0309	20.11	10.22	9.96	9.64	9.85	9.41	10.46
10439299	Stfa3	0.0323	18.98	3.38	3.11	3.01	3.26	3.16	3.48
10593332	Bco2	0.0323	6.45	7.57	7.80	7.82	7.61	7.39	6.91
10606989	Tsc22d3	0.0329	12.34	7.57	7.56	8.17	8.38	8.35	7.75
10416689	Olfm4	0.0340	7.39	7.78	8.07	8.18	8.17	7.87	6.98
10394735	Pdia6	0.0340	19.14	10.76	10.55	10.41	10.58	10.87	11.01
10484201	2610301F02Rik	0.0341	18.87	9.09	8.88	8.80	8.95	8.99	9.47
10556463	Arntl	0.0361	18.97	8.36	7.76	7.45	8.05	7.28	8.63
10485241	Accs	0.0380	6.59	6.37	6.67	6.68	6.48	6.18	6.22
10544837	1200009O22Rik	0.0384	21.37	7.57	7.28	7.10	7.16	6.81	7.57
10574087	Herpud1	0.0396	9.82	11.11	11.35	11.59	11.64	11.90	10.97
10371482	Hsp90b1	0.0404	18.41	11.69	11.55	11.47	11.61	11.99	11.98
10417734	Nr1d2	0.0429	6.97	8.35	8.82	9.06	8.74	9.18	7.65
10424979	Gpt	0.0448	8.30	6.50	6.71	6.93	6.80	6.93	6.40
10545041	Nap1l5	0.0452	6.07	7.49	7.80	7.76	7.49	7.00	7.11
10462132	Pgm5	0.0452	7.85	8.65	8.97	9.33	9.04	8.85	8.09
10378816	Slc6a4	0.0455	6.97	6.91	7.27	7.24	7.04	7.19	6.54
10411622	Birc1f	0.0492	13.22	3.44	3.40	3.70	4.10	3.68	3.55
10383767	Osbp2	0.0493	7.12	7.50	7.77	7.77	7.72	7.56	6.97
10360563	Smyd3	0.0495	6.24	7.75	7.88	7.94	7.76	7.62	7.51
10381445	Tmem106a	0.0502	6.35	9.15	9.47	9.38	9.25	9.10	8.96
10426425	Pdzrn4	0.0502	22.83	5.93	5.72	5.54	5.45	5.51	5.80
10363773	Rhobtb1	0.0506	18.62	9.25	9.02	8.85	9.16	9.11	9.36
10602865	Pdha1	0.0512	7.83	8.19	8.38	8.41	8.38	8.36	7.99
10471586	Hspa5	0.0512	15.61	11.42	11.31	11.38	11.77	12.28	11.61
10420114	Tgm1	0.0512	10.05	7.83	8.09	8.22	8.51	8.65	7.61
10584712	Hyou1	0.0512	16.57	9.40	9.26	9.24	9.63	10.23	9.68
10597960	Slc6a20a	0.0541	9.40	7.96	8.12	8.47	8.36	8.02	7.95
10356484	Gbx2	0.0549	23.25	6.16	6.04	5.81	5.77	5.84	6.09

10425601	Tef	0.0549	8.95	8.67	8.92	9.29	9.29	9.40	8.42
10408838	Elovl2	0.0549	19.76	8.75	8.37	8.18	8.31	8.29	9.12
10566258	Hbb-b1	0.0551	3.65	12.68	12.91	12.61	12.29	12.71	12.38
10409666	Kif27	0.0551	21.04	4.95	4.85	4.63	4.70	4.70	5.11
10514520	Cyp2j9	0.0551	7.19	7.50	7.89	7.84	7.84	7.79	7.30
10556553	Insc	0.0560	19.81	6.57	6.27	6.24	6.31	6.26	6.70
10395039	Cmpk2	0.0560	18.12	7.23	7.06	7.00	7.19	7.16	7.41
10566254	Hbb-b1	0.0560	3.67	12.69	12.91	12.62	12.31	12.73	12.38
10563314	Dhdh	0.0561	8.77	6.83	7.12	7.27	7.22	7.32	6.78
10447341	Rhoq	0.0592	8.21	7.33	7.60	7.68	7.63	7.43	7.17
10452815	Xdh	0.0592	11.24	7.80	8.03	8.18	8.35	8.03	7.94
10375704	3010026O09Rik	0.0597	2.55	8.29	8.38	8.14	7.98	7.70	8.11
10402195	Tc2n	0.0608	9.25	5.39	6.27	6.45	6.60	6.96	5.09
10538658	Herc3	0.0643	6.83	8.59	9.12	9.19	8.90	8.64	8.43
10530201	Ugdh	0.0654	7.77	10.72	10.84	11.04	10.84	10.77	10.51
10597758	Csrnp1	0.0654	10.62	6.44	6.66	6.86	7.05	6.78	6.52
10500555	Hsd3b3	0.0655	8.30	8.79	9.04	9.21	9.32	9.52	8.23
10347481	Cyp27a1	0.0655	8.38	8.59	8.93	8.98	8.98	9.01	8.22
10351491	Olfml2b	0.0655	23.10	6.24	5.97	5.76	5.74	5.58	6.05
10414970	A730076H11Rik	0.0655	22.59	5.74	5.40	5.30	5.07	4.75	5.68
10385893	Slc22a4	0.0655	7.40	9.06	9.19	9.43	9.17	9.24	8.64
10426098	Creld2	0.0656	14.27	8.02	8.09	8.16	8.72	9.26	8.23
10568709	Clrn3	0.0656	20.15	9.84	9.62	9.57	9.57	9.63	9.98
10504203	4930578G10Rik	0.0676	11.73	5.23	5.72	5.79	6.19	6.08	5.58
10435048	Tctex1d2	0.0690	6.23	7.46	7.56	7.74	7.47	7.30	7.26
10436636	Ncam2	0.0690	7.32	4.03	4.25	4.38	4.24	4.27	3.91
10596454	Alas1	0.0690	12.76	10.36	10.39	10.62	11.14	11.34	10.43
10526853	Fam20c	0.0706	18.79	8.96	8.81	8.74	8.89	9.04	9.09
10521391	Acox3	0.0708	8.41	9.98	10.16	10.33	10.36	10.44	9.64
10587780	Tuba1b	0.0732	19.24	11.25	10.98	10.95	11.09	11.18	11.44
10578690	Neil3	0.0732	20.96	5.27	4.71	4.62	4.67	4.59	5.40
10423548	Sdc2	0.0732	7.68	9.01	9.34	9.31	9.33	9.35	8.69
10556583	Nucb2	0.0736	8.18	7.90	8.06	8.17	8.08	8.18	7.82
10549222	Bcat1	0.0738	5.86	8.99	8.98	9.08	8.88	8.47	8.42
10386844	Zswim7	0.0757	7.47	8.32	8.55	8.62	8.49	8.48	8.18
10549108	Abcc9	0.0757	8.81	8.01	8.32	8.43	8.44	8.25	7.66
10544525	Pdia4	0.0758	16.97	10.14	10.02	10.01	10.27	10.64	10.36
10405755	---	0.0765	20.89	7.91	7.71	7.41	7.61	7.94	8.05
10522208	Uchl1	0.0765	7.18	6.10	6.37	6.55	6.27	6.13	6.06
10592449	Olfr149	0.0765	0.62	5.41	5.20	5.08	4.87	5.28	5.13
10574572	2210023G05Rik	0.0769	6.63	7.20	7.40	7.35	7.33	7.09	6.76
10544588	Gimap3	0.0775	10.34	4.82	4.88	5.13	5.34	4.95	4.63
10435791	---	0.0777	8.09	7.82	8.19	8.19	8.16	8.20	7.81
10356240	Slc16a14	0.0784	13.54	8.78	9.01	9.06	9.60	10.07	9.09
10432398	Tuba1b	0.0790	19.35	10.96	10.73	10.69	10.82	10.86	11.17
10565819	Slco2b1	0.0798	11.91	7.53	7.70	7.87	8.12	8.21	7.71
10363173	Gja1	0.0810	8.57	6.68	6.93	7.07	6.92	6.98	6.66
10545086	Snca	0.0810	3.79	6.91	7.08	6.95	6.66	6.75	6.75
10501608	Vcam1	0.0810	13.07	7.15	7.27	7.39	7.60	7.90	7.34
10504137	4933409K07Rik	0.0810	12.57	7.07	7.12	7.31	7.71	7.93	7.17
10504201	4933409K07Rik	0.0810	12.57	7.07	7.12	7.31	7.71	7.93	7.17
10512350	4933409K07Rik	0.0810	12.57	7.07	7.12	7.31	7.71	7.93	7.17
10512352	4933409K07Rik	0.0810	12.57	7.07	7.12	7.31	7.71	7.93	7.17
10359113	Fam163a	0.0810	17.19	7.43	7.31	7.22	7.54	7.46	7.65
10597592	Acaa1b	0.0810	9.41	9.17	9.39	9.47	9.48	9.45	9.12
10460072	Cndp1	0.0810	8.25	9.22	9.23	9.58	9.49	9.18	8.78
10558961	Tspan4	0.0810	9.90	8.32	8.63	8.89	8.89	9.34	8.39
10542953	Tfpi2	0.0810	21.14	8.97	8.73	8.61	8.59	8.40	9.00
10512739	Xpa	0.0821	4.52	7.90	8.08	8.06	7.74	7.47	7.80
10592058	Tuba1b	0.0824	19.01	10.96	10.71	10.70	10.85	10.92	11.16
10544932	Inmt	0.0824	8.53	12.37	12.51	12.80	12.72	12.89	11.79
10395389	Sostdc1	0.0825	22.36	10.55	10.33	10.21	10.09	9.95	10.67
10449452	Fkbp5	0.0825	11.84	8.40	8.55	8.87	9.36	9.62	8.52
10529824	Prom1	0.0849	20.71	8.92	8.69	8.53	8.46	8.23	9.15
10390691	Nr1d1	0.0849	4.35	8.60	8.72	8.51	7.82	7.55	7.49
10441718	Park2	0.0849	7.79	6.55	6.58	6.82	6.75	6.52	6.23
10562548	C80913	0.0849	6.55	8.21	8.43	8.49	8.28	8.33	8.15
10349932	Etnk2	0.0859	8.75	5.35	5.65	5.88	5.80	5.99	5.29
10349571	Fcamr	0.0865	7.42	7.74	8.09	8.24	7.97	7.13	6.71
10503497	Slc7a13	0.0874	9.28	12.11	12.33	12.47	12.46	12.55	11.98
10545877	Cml4	0.0874	8.95	9.60	9.69	10.10	10.38	10.71	8.77
10391649	Slc4a1	0.0880	20.45	8.32	8.19	8.09	8.07	7.93	8.49

10527936	Fzd1	0.0880	0.12	9.14	9.05	8.91	8.74	8.79	9.03
10504375	Npr2	0.0889	7.53	7.27	7.67	7.67	7.59	7.60	7.14
10597817	Cck	0.0903	17.20	7.44	7.08	7.22	7.46	8.00	7.51
10519555	Abcb1b	0.0903	5.26	7.43	7.69	7.64	7.27	6.08	7.16
10364222	Ftcd	0.0906	8.59	6.94	7.20	7.34	7.33	7.56	6.47
10471737	---	0.0908	22.98	3.03	2.90	2.73	2.70	3.24	2.95
10431872	Slc38a1	0.0908	21.02	4.95	4.67	4.64	4.55	4.34	5.18
10455457	Npy6r	0.0909	16.47	4.85	4.56	4.64	5.18	4.32	5.14
10598863	Rgn	0.0914	7.02	5.73	5.92	5.96	5.82	5.61	5.40
10518781	Per3	0.0926	8.31	5.93	6.39	6.77	6.62	7.06	5.83
10426650	Tuba1c	0.0926	19.25	10.94	10.72	10.67	10.81	10.88	11.13
10535904	Hsph1	0.0934	14.13	9.94	9.84	10.03	10.36	10.85	10.01
10409278	Nfil3	0.0934	17.33	7.58	7.18	7.22	7.84	7.37	8.09
10412345	Parp8	0.0934	7.80	8.14	8.32	8.34	8.32	8.22	7.89
10447921	---	0.0934	7.23	2.47	2.59	2.70	2.54	2.45	2.27
10488029	Zfand1	0.0934	5.57	9.39	9.47	9.53	9.30	9.09	9.15
10575867	Mlycd	0.0967	8.48	7.28	7.49	7.58	7.50	7.44	7.20
10497636	---	0.0967	3.24	7.57	7.68	7.59	7.23	6.90	7.41
10355205	D630023F18Rik	0.0967	0.34	10.44	10.34	10.17	10.03	9.86	10.33
10466304	Dtx4	0.0967	20.61	8.45	8.21	7.79	7.98	7.69	8.52
10514221	Plin2	0.0967	6.93	9.95	10.04	10.10	9.99	10.12	9.70
10428338	Dpys	0.0967	7.44	8.10	8.34	8.46	8.30	7.77	7.59
10399198	Ncoa4	0.0967	10.68	10.32	10.41	10.55	10.59	10.64	10.32
10347741	Mogat1	0.0972	7.81	9.56	9.80	9.90	9.98	9.95	8.41
10525439	P2rx4	0.0973	6.57	8.87	9.02	8.97	8.94	8.80	8.63
10422244	Slitrk6	0.0974	9.96	4.82	5.19	5.41	5.76	5.55	4.72
10380524	Slc35b1	0.0976	17.78	9.03	8.84	8.81	9.08	9.35	9.20
10518532	Tardbp	0.0977	16.86	9.23	9.08	9.13	9.32	9.51	9.37
10526363	Por	0.0978	8.76	10.51	10.63	10.74	10.74	10.78	10.31
10509204	Tcea3	0.0984	6.66	8.87	8.97	8.98	8.95	8.79	8.62
10480003	Itih2	0.0987	8.39	6.62	7.04	7.05	7.09	7.11	6.08
10355954	BC035947	0.0989	8.33	8.18	8.62	8.59	8.69	8.55	7.53
10523128	Ppbp	0.0995	3.39	5.89	6.12	5.35	5.20	5.63	4.97
10553403	Htatip2	0.0995	7.54	7.46	7.78	7.74	7.74	7.60	7.04

Supplementary Table 3. Differentially expressed transcripts between *clock*-knockout and wild-type mice with a FDR<10% and a fold change > 50%.

				Average Expression
Probe ID	**Symbol**	**FDR**	**Fold Change**	**A-value**
10604576	Gpc3	0.0000	1.72	8.54
10500570	Hao2	0.0000	2.07	11.04
10506125	Angptl3	0.0000	1.89	7.64
10519555	Abcb1b	0.0000	2.07	6.88
10531149	Gc	0.0000	2.16	10.25
10531073	Ugt2b38	0.0000	-13.36	10.04
10445293	Pla2g7	0.0000	1.92	8.85
10367059	BC089597	0.0001	1.72	9.99
10522335	Atp10d	0.0001	2.27	7.69
10467897	Cyp2c44	0.0001	1.65	9.52
10531034	Ugt2b34	0.0001	1.75	9.30
10423030	Prlr	0.0001	2.94	7.76
10580635	Ces3	0.0001	-1.92	10.79
10531057	Ugt2b5	0.0001	-2.59	8.19
10535841	Slc46a3	0.0001	-1.70	8.14
10498981	Fgb	0.0001	1.89	6.42
10467887	Cpn1	0.0001	1.57	9.99
10438769	Cldn1	0.0001	1.62	7.95
10490867	Slc7a12	0.0001	5.34	9.46
10355717	Slc23a3	0.0001	1.53	6.99
10396831	Arg2	0.0001	2.04	6.59
10607738	Car5b	0.0001	1.54	10.80
10545874	Cml5	0.0001	-6.06	7.70
10423049	Prlr	0.0001	3.31	7.39
10502240	Npnt	0.0002	1.52	9.77
10512895	Baat	0.0002	1.65	5.83
10389894	Abcc3	0.0004	1.61	6.18
10439068	Osta	0.0004	-1.83	8.26
10556769	Acsm3	0.0004	-1.59	11.64
10366707	Avpr1a	0.0004	1.65	8.62
10492735	Fgg	0.0005	2.68	7.52
10364784	Reep6	0.0005	-1.54	8.69
10523062	Alb	0.0005	-1.96	6.32
10581664	Il34	0.0006	-1.55	7.51
10436967	Cbr1	0.0008	1.51	9.40
10402195	Tc2n	0.0008	-1.80	6.36
10452879	Nlrc4	0.0009	-1.56	5.25
10467110	AI747699	0.0010	-1.53	8.91
10499906	Smcp	0.0011	-1.77	6.43
10578904	Cpe	0.0013	-1.75	8.50
10507152	Cyp4a12b	0.0015	-3.19	8.47
10545865	Cml3	0.0015	-1.97	10.17
10581865	Ldhd	0.0016	-1.64	10.91
10466659	Gda	0.0016	-1.60	6.29
10545869	Cml3	0.0016	-1.99	10.17
10545877	Cml4	0.0017	-1.81	10.10
10545862	Cml3	0.0018	-1.98	10.26
10548879	Mgp	0.0018	-1.66	9.02
10515187	Cyp4a14	0.0018	2.51	10.27
10465753	D630002G06Rik	0.0022	1.83	7.09
10516064	Mfsd2	0.0024	-1.67	8.57
10465726	BC014805	0.0024	-2.23	7.42
10363224	Fabp7	0.0025	1.81	7.04
10500360	Gm15441	0.0029	-2.04	6.00
10551226	Cyp2a4	0.0029	-3.51	10.18
10471912	Kynu	0.0029	1.76	8.17
10507143	Cyp4a12a	0.0040	-3.93	8.13
10371400	Cry1	0.0070	1.60	7.15
10362458	Trdn	0.0071	-1.68	3.68
10490989	Cp	0.0073	1.51	9.06
10548207	Pzp	0.0076	-2.47	8.50
10496001	Cfi	0.0079	1.64	7.05
10402390	Serpina1b	0.0084	-1.83	6.97
10365290	Chst11	0.0085	-1.50	7.67
10495035	Slc16a1	0.0090	1.57	9.51
10427436	C7	0.0092	-1.50	7.53
10551282	LOC100047728	0.0098	-2.49	9.77

10531061	Ugt2b37	0.0102	-2.48	9.90
10531066	Ugt2a3	0.0181	2.10	7.03
10347741	Mogat1	0.0200	-1.50	9.80
10548978	Slco1a1	0.0228	-3.09	9.47
10556463	Arntl	0.0246	1.95	7.69
10382189	Apoh	0.0281	-1.60	6.16
10417734	Nr1d2	0.0316	-1.54	8.71
10497381	Cyp7b1	0.0399	-2.22	10.57
10514478	Cyp2j13	0.0657	-1.76	10.77
10373452	Gm129	0.0797	-2.10	5.96
10490913	Car3	0.0811	-1.59	9.36
10345675	Npas2	0.0832	1.66	7.07

fold change was calculated as the ratio of the maximal to minimal transcript abundance across the 24-hour circadian cycle.

Supplementary Table 4. KEGG pathway enriched among genes differentially expressed in *clock*-knockout mice.

KEGG Pathway	Count	Fold Enrichment	FDR	Genes
Retinol metabolism	7	15.37	0.0002	Cyp4a12b, Cyp4a12a, Cyp2c44, Ugt2b34, Ugt2b5, Ugt2a3, Cyp4a14
Arachidonic acid metabolism	6	10.81	0.0039	Cyp4a12b, Cyp2j13, Cbr1, Cyp4a12a, Cyp2c44, Cyp4a14
Porphyrin and chlorophyll metabolism	4	18.74	0.0157	Ugt2b34, Ugt2b5, Cp, Ugt2a3
Complement and coagulation cascades	5	9.49	0.0171	C7, Fgg, Serpina1b, Fgb, Cfi
Circadian rhythm	3	32.43	0.0296	Npas2, Arntl, Cry1
Steroid hormone biosynthesis	4	12.49	0.0254	Cyp7b1, Ugt2b34, Ugt2b5, Ugt2a3
Drug metabolism	4	12.22	0.0232	Ces3, Ugt2b34, Ugt2b5, Ugt2a3
Ascorbate and aldarate metabolism	3	28.11	0.0248	Ugt2b34, Ugt2b5, Ugt2a3
Pentose and glucuronate interconversions	3	24.80	0.0282	Ugt2b34, Ugt2b5, Ugt2a3
Metabolism of xenobiotics by cytochrome P450	4	8.65	0.0424	Cyp2c44, Ugt2b34, Ugt2b5, Ugt2a3
Drug metabolism	4	7.70	0.0527	Cyp2c44, Ugt2b34, Ugt2b5, Ugt2a3
PPAR signaling pathway	4	7.40	0.0538	Cyp4a12b, Cyp4a12a, Fabp7, Cyp4a14
Androgen and estrogen metabolism	3	12.78	0.0698	Ugt2b34, Ugt2b5, Ugt2a3
Starch and sucrose metabolism	3	11.71	0.0762	Ugt2b34, Ugt2b5, Ugt2a3
Fatty acid metabolism	3	10.04	0.0942	Cyp4a12b, Cyp4a12a, Cyp4a14

Supplementary Table 5. Nucleotide sequence homology between Cyp4a12a, Cypça12b, Cyp4a14 and other members of the CYP family*.

	Cyp4a12a	Cyp4a12b	Cyp4a14
	% identity	% identity	% identity
Cyp4a12a	100	98	78
Cyp4a12b	98	100	78
Cyp4a14	78	78	100
Cyp4a10	81	81	
Cyp4a32	80	80	
Cyp4a31	80	80	
Cyp4a29	77	77	77
Cyp4a14-like	83	82	85

* -only sequences with >75% of identity have been introduced in the Table.